Ca' Foscari
University
of Venice

DEPARTMENT OF MOLECULAR SCIENCES AND NANOSYSTEMS

Master's Degree Thesis in

*Sustainable Chemistry and*

*Technologies*

**Hydrosilylation of alkenes and alkynes**

**with Pt(II)-based catalysts and application of Machine Learning algorithms**

**to optimize the reduction of amides to amines**

***Supervisor***
Ch. Prof. Steven P. Nolan
Ch. Prof. Fabiano Visentin

***Candidate***
Eleonora Casillo

***Assistant supervisor***
MSc Benon Maliszewski
Ch. Dott. Thomas Scattolin

***Academic year***
2023/2024

*To my brother Matteo*

*And my boyfriend Amedeo*

*"The best thing to do when you're being sad" replied Merlin "is to learn something. That's the only thing that never fails. You may grow old and trembling in your anatomies, you may lie awake at night listening to the disorder of your veins, you may miss your only love, you may see the world about you devastated by evil lunatics, or know your honour trampled in the sewers of baser minds. There is only one thing for it then — to learn. Learn why the world wags and what wags it. That is the only thing which the mind can never exhaust, never alienate, never be tortured by, never fear or distrust, and never dream of regretting. Learning is the only thing for you. Look what a lot of things there are to learn."*

*T.H. White, The Once and Future King*

# Index

# *Abstract*

This master thesis is split in two big paragraphs: the first one regarding the Hydrosilylation of alkenes and alkynes with seven different Pt(II)-based catalysts, meanwhile the second section is about the application of Machine Learning (ML) method in chemistry in order to optimize reaction conditions limiting the waste of time, chemicals and money. The Hydrosilylation of alkenes and alkynes, that is, the addition of silanes across carbon–carbon double or triple bonds, represents the ideal pathway to produce organosilicon compounds, thus, it is hardly surprising that this transformation constitutes the core of the organosilicon industry in order to produce various silicon compounds ranging from bulk commodities to fine chemicals and specialty products, for example, lubricating oils, paper release coatings, or grafting agents. Furthermore, the organosilane products serve as valuable foundational components for organic synthesis, by taking advantage of the richness and versatility of organosilicon chemistry. Concerning my project, first of all two simple [Pt(thioether)$_2$Cl$_2$] pre-catalysts were synthesized starting from PtCl$_2$ or K$_2$[PtCl$_4$] and Tetrahydrothiophene (THT) or Dimethyl sulfide (DMS). Then, these two catalysts and other five were used for the hydrosilylation in different loadings (mol%). The other five catalysts ([Pt(IPr)(DMS)Cl$_2$], [Pt(SIPr)(DMS)Cl$_2$], [Pt(IMes)(DMS)Cl$_2$], [Pt(IPr*)(DMS)Cl$_2$] and [Pt(ICy)(DMS)Cl$_2$]) are all based on [Pt(DMS)Cl$_2$] and the fourth ligand is an *N*-heterocyclic carbene. Their catalytic activity was studied with Gas Chromatography and $^1$H-NMR, by calculating the yield and the conversion of the substrate into the desired product. The catalysts that were used for the hydrosilyaltion are the same that were employed in the second section of the project: the optimization of the reduction of amides to amines. The optimization of chemical reactions is often guided by empirical methods, it means that chemists engage in testing operational parameters that, according to their understanding of the reaction, are expected to yield optimal results. This approach can be time and resource-intensive, given that slight adjustments to various factors can significantly impact production. Machine Learning (ML) enables the creation of complex patterns between the different process variables and quickly pinpoints the optimal operation point while guiding a smart and efficient experimental campaign. *Sunthetics* ML is an easy-to-use machine learning (ML) platform that helps you develop new materials, processes, and formulations using very few data points to accurately predict your system's behavior. The chemical industry has become the third largest contributor of greenhouse gas emissions, with more than half of its resources ending

up in waste streams. *Sunthetics'* mission is make the chemical industry more sustainable, one reaction at a time. The reaction that was tried to be optimized in this project by using the algorithms suggestions was the reduction of amides to amines and, from reading the results, it was possible to confirm that the algorithm had proposed the reaction with the most optimal conditions already in the second set of suggested reactions.

# Project 1

*Hydrosilylation of alkenes and alkynes with Pt-thioether-based and Pt-NHC-based catalysts*

# Chapter 1

## Synthesis of N-heterocyclic carbene complexes and their application

## 1.1 Introduction

*N*-Heterocyclic carbenes (NHCs) are a subclass of carbenes[1] that represent a significant group of organic compounds characterized by a heterocyclic ring incorporating at least one nitrogen atom within its structure. (Figure 1).[2]
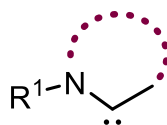


*Figure 1: general structure of an NHC.*

NHCs own a distinctive feature that sets them apart from other classes of carbenes: they are neutral molecules of general formula of R1-(C:)-R2, consisting of a divalent carbon atom possessing two non-bonding electrons.[3] They are known for their ability to form stable complexes with a wide range of metal centers, and they have found extensive use in organometallic chemistry and catalysis.[4] Due to their uncommon properties and to the fact that they are easy to synthesize and offer so many

different options to functionalize them, NHCs have been used over the years in several applications across different fields such as catalysis, organic synthesis, materials science, for example for coordination polymers with interesting electronic and optical properties that can have applications in electronics, optoelectronics, and photovoltaics.[5] NHCs have shown potential in medicinal chemistry as well, as ligands for metal-based drugs or as active pharmaceutical ingredients. They can enhance the stability and efficacy of metal complexes used in chemotherapy or antimicrobial agents.[6] In the next paragraph there is an exhaustive description of the history of NHCs, the explanation about the structure of this class of compounds and their electronic and steric properties and lastly is described the synthesis of various novel well-defined Pt-based NHC complexes and their catalytic properties.

## 1.2 Historical aspects

The idea of carbenes traces back to the late 19th century, and for a considerable period, they were merely hypothesized to serve as transient intermediates participating in some organic reactions.[7] Prior to 1960, the belief prevailed that carbenes, due to their high reactivity, could not be isolated, thus hindering extensive exploration in the field of carbene chemistry.[8][9] It may be true for the majority of carbenes; however, this is not accurate for *N*-heterocyclic carbenes. In 1962, Wanzlick made the first in-depth study on the stability and reactivity of NHCs and in 1968 Wanzlick and Schönherr reported the first application of metal-NHC chemistry.[10] Unexpectedly, the interest about NHCs remained asleep for the next twenty years.[9] In the 1960s, Ernst Otto Fischer and Richard R. Schrock made significant contributions to the field of NHCs; Fischer is credited with the synthesis and characterization of the first stable NHC, which was a six-membered ring with nitrogen and carbon atoms. Schrock contributed to the understanding of NHCs' reactivity and their role in organometallic chemistry. In 1991, Anthony J. Arduengo reported the synthesis of the first stable NHC with a bulky substituent (adamantyl group) with sufficient kinetic and thermodynamic stability to be easily isolated and characterized, making NHCs more practical for use in catalysis.[2] The deprotonation of 1,3-di-1-adamantylimidazolium chloride in THF at room temperature with catalytic sodium methylsulfinylmethylide [($^-$CH$_2$S(O)CH$_3$)Na$^+$] in the presence of 1 equivalent of sodium hydride (NaH) produces carbene **1** (Figure 2). This deprotonation can also be carried with potassium *tert*-butoxide in THF, resulting in a 96% yield of **1**.[2] The resulting carbene is unstable in the presence of oxygen

and moisture, because it re-protonates immediately due to the presence of the very reactive carbon. This bulky NHC, known as the "*Arduengo carbene"*, significantly enhanced the stability and applicability of NHCs in various chemical reactions.[11]
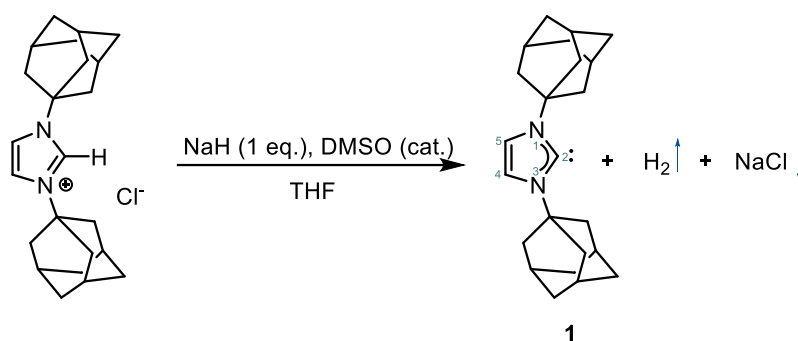


*Figure 2 : Synthesis of N,N-bis-(adamantyl)imidazol-2-ylidene.* [2]

A single crystal suitable for X-ray diffraction studies was grown by cooling a toluene solution of **1** (Figure 2). The significant steric bulk offered by the adamantyl substituents in **1** undoubtedly contributes to the kinetic stability. The electronic effects that stabilize Arduengo carbene arise from the ability of nitrogen atoms to provide electronic density through π interactions. These effects, combined with the steric bulk of the adamantyl groups, make the carbene relatively stable. After this discovery, it was still unclear whether electronic or steric effects lay at the origin of the surprising stability of the carbene. It was hypothesized that the bulky adamantyl group shielded the carbene as shown in the Figure 3.[2] A following publication of Arduengo reported four additional free carbenes, including Me$_2$IMe, which has much smaller *N*-substituents, suggesting that the carbene stabilization is rather electronic than steric. The electronic stabilization factors include π-donation into the carbene's out-of-plane *p* orbital by the electron-rich π-system (N—C=C—N). These π-interactions create different effective resonance structures for compound **1**, where the positive charge is delocalized within the imidazole ring, and C$_2$ is depicted as a π-bonded carbanionic center. Additional stability for the carbene's electron pair comes from the σ-electronegativity effects of the nitrogen atoms on the carbene center: nitrogen atoms are more electronegative than carbon, which means

they tend to withdraw electronic density from carbon. This effect helps to better distribute the negative charge, further stabilizing the carbene center.[11] The peculiar stability of these carbenes is explored further in the paragraph 1.3.
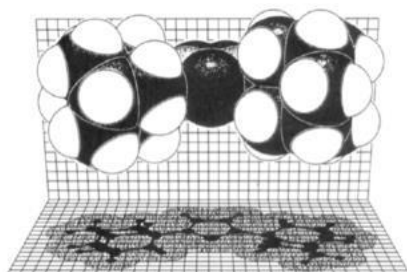


Figure 3 : Space-filling kanvas1 drawing of the X-ray structure of the Arduengo carbene.[11]

In the early stages of their discovery, NHCs were initially regarded as alternative two-electron donor ligands to phosphines.[12] However, it soon became apparent that NHCs exhibit stronger σ-electron-donating properties compared to phosphine ligands,[13] although with minimal differences. [14,15] In fact, in 1991, when Arduengo isolated and "*bottled*" the first NHC, it marked the synthesis of competitive alternatives to phosphines in the realm of organometallic chemistry. NHC complexes often provide better catalytic performances than phosphines and greater stability to air and moisture.[5] This realization quickly established NHCs as a superior choice as ancillary ligands for transition metal-catalysis, due to their ability to form stronger bonds with metal centers,[16] either in their low or high valence states. This characteristic gives rise to transition metal complexes that are generally highly stabilized and resistant to decomposition, resulting in higher turnover numbers of the catalyst, without requiring an excess of ligand, as conventionally practiced with phosphines. Therefore, their peculiar σ-basic/π*-acidic properties combined with their ability to stabilize reactive metal centers, make transition metal-NHC complexes valuable (pre)catalysts for many homogeneous catalyzed transformations.[17] [18] NHCs are used as organo-catalysts in various reactions. In recognition of their pioneering work in the development of the metathesis method in organic synthesis, Yves Chauvin, Robert H. Grubbs, and Richard R. Schrock were jointly awarded the Nobel Prize in Chemistry in 2005.[19]
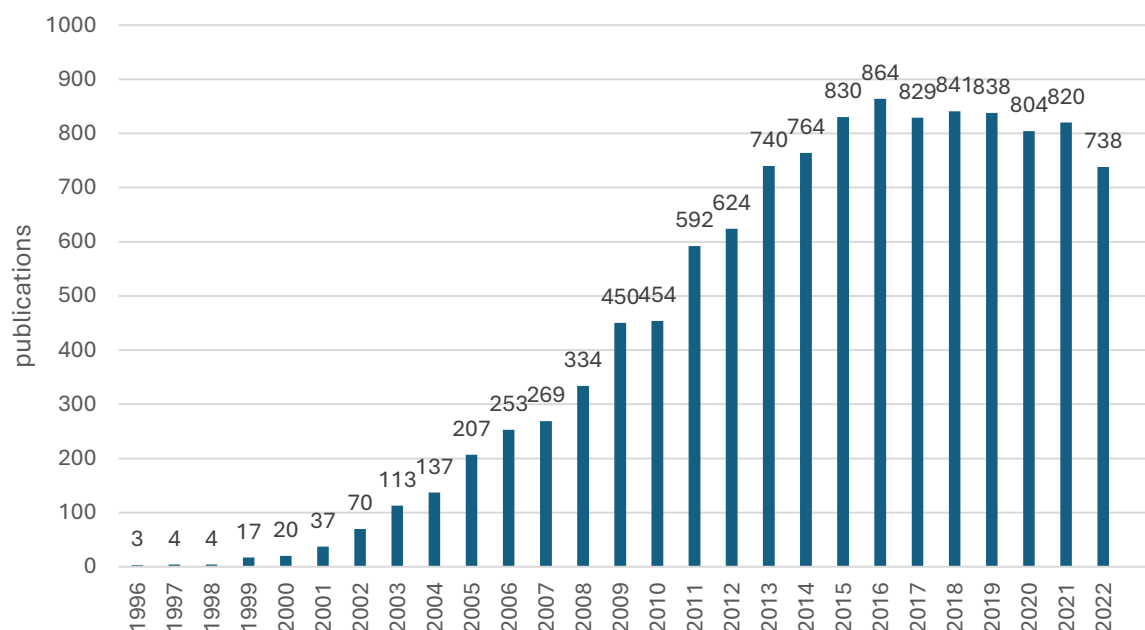
*Figure 4: Number of publications using N-Heterocyclic carbenes per year in ISI WEB OF SCIENCE database.*

Research in the field of *N*-heterocyclic carbenes continues to advance, with new NHC ligands being designed and synthesized to improve catalytic efficiency and selectivity.[20] NHCs are nowadays used in various fields, including pharmaceuticals, materials science, and green chemistry, due to their versatility and stability. Over the past few years, the NHCs chemistry has been a field of vivid scientific competition and yielded previously unexpected successes, mostly in the areas of homogeneous catalysis. From the work in numerous academic laboratories and in industry, a revolutionary turning point in organometallic catalysis is emerging.[1] It is clear how in the recent years the interest for of *N*-heterocyclic carbenes has grown if we look at the graph reported in Figure 4: it shows the number of publications written about *N*-heterocyclic carbenes over the years, and clearly there has been a huge growth in the last three decades (from 1996 to 2022).

# 1.3   Stability of NHCs

In NHCs the carbene carbon atom is bound to at least a nitrogen atom within a heterocyclic ring structure (Figure 5), which contributes to their peculiar stability and reactivity.
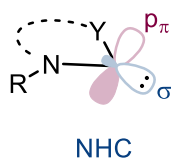


*Figure 5: Minimal structural requirement for an N-heterocyclic carbene.*

Caused by the strong back-bonding to the carbene carbon from the nitrogen atoms, it significantly reduced the necessity of back-bonding from the metal center, so much so that, very often, NHCs serve as strong σ-donors (Figure 6).
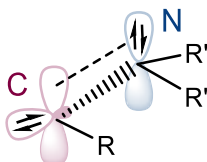


*Figure 6: interactions between the carbene carbon, the metal center and the N atoms*

Indeed, due to their incomplete octet and coordinative unsaturation, carbenes are inherently reactive and unstable species. Nevertheless, classical imidazol(id)in-2-ylidene NHCs exhibit an unusual stability due to the presence of two p-electron donating nitrogen atoms adjacent to the carbene carbon (Figure 7), which allows for delocalization and p-donation into the formally vacant $p_\pi$-orbital of the carbene carbon.
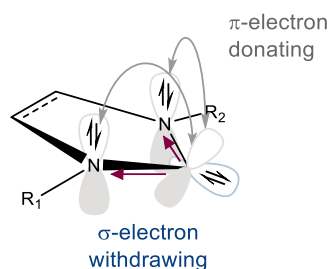
*Figure 7: The inductive (purple arrows) and mesomeric (grey arrows) electronic stabilization of imidazol(id)in-2-ylidene NHCs.*

NHCs are primarily employed as ligands for transition metals, categorized as conventional σ-basic/π*-acid ligands, whose electronic properties can be elucidated through the molecular orbital diagram depicted in Figure 8.
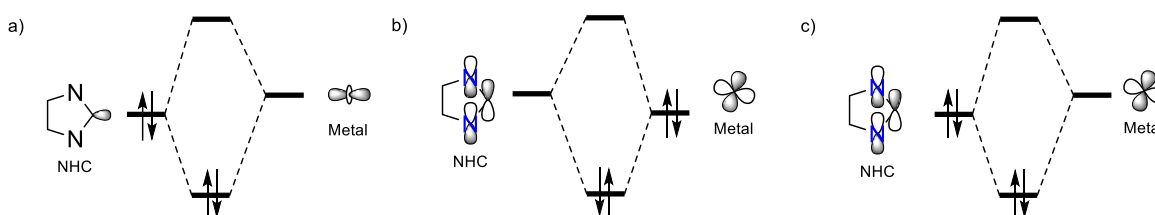


*Figure 8: Diagram illustrating the σ→d (a), the d→π* (b), and the π→d (c) bonding modes occurring between NHCs and transition metals.*

The NHC presents a lone pair of electrons in a high energy $\sigma$ orbital, which confers to NHCs a stronger $\sigma$ donation property (basicity) than that of even basic phosphines, such as tricyclohexylphosphine (PCy$_3$), leading to a strong metal-carbon bond in transition metal complexes, thus also influencing the metal center's proprieties as shown in Figure 8a. The strong $\sigma$-donating properties of NHCs are used to electronically stabilize highly reactive organometallic species.[21] Strong NHC-metal bonds stabilize many reactive organometallic intermediates that cannot be fully characterized using analogous phosphine complexes.[22] In addition, NHCs exhibit greater thermal stability to phosphines as

7

the P-C bond can undergo degradation at elevated temperatures. With empty low-energy $\pi^*$ orbitals, NHCs are allowed to act as acceptors of electron density from filled $d$ orbitals ($\pi$-acidity) of metals in a classical $d{\rightarrow}\pi^*$ back-donation (Figure 8b). Finally, when paired with electron-deficient metals, NHCs can engage in a $\pi{\rightarrow}d$ donation process, in which the combination of filled and empty $\pi$ orbitals on the NHC donate electron density to the empty $d$ orbitals of the metal ($\pi$-basicity) (Figure 8c).[23] This description of M-NHC bonding has been developed over several years of research, since NHC ligands were initially considered to be pure $\sigma$-donors with insignificant $\pi$- acidity capability. Thus, the principal use of NHCs was as ancillary ligands in transition metal catalyzed homogeneous reactions as octet defiant species,[24] that truly propelled the widespread popularity of NHCs.[5,20] In the early 20th century, NHCs have become hugely popular ligands in transition metal catalysis.

In addition, the higher electronegativity of nitrogen compared to carbon exerts a negative inductive effect, withdrawing electron density from the carbene carbon center and thereby stabilizing the σ-orbital. Atoms or groups with a negative inductive effect are more electronegative than the carbon atom they are attached to, which means they have a stronger pull-on electron. This stronger pull results in a partial positive charge (δ+) on the carbon atom to which they are attached and a partial negative charge (δ-) on themselves. The inductive effect arises from the σ electron-withdrawing properties of the adjacent nitrogen atoms, this lowers the electron density on the carbene carbon.[25] The mesomeric effect on the other hand allows for π-delocalization of the nitrogen lone pair.[26] This delocalization arises from the interaction of the filled $p$ orbitals of the $N$-atoms and the empty $p$ orbital of the carbene carbon, this is $p\pi$-$p\pi$ delocalization. Both effects are visualized using the imidazolylidene carbene (Figure 7). Thus, the negative inductive effect combined with the positive mesomeric effect on the carbene carbon provide a substantial energy gap between the HOMO σ-orbital and the LUMO pπ-orbital ($\geq$ 2 eV), which is a pivotal factor for attaining a stable singlet carbene.[17] Singlet carbenes have two electrons with opposite spins in their highest occupied molecular orbital (HOMO), making them electronically stable, at least for a short period of time.[1] The positive mesomeric effect occurs when a substituent or functional group donates electrons through resonance to a conjugated system. The positive mesomeric effect in N-heterocyclic carbenes arises from the ability of the lone pair electrons on the nitrogen atoms to participate in resonance or mesomeric structures. This means that these electrons can be delocalized or shared with the adjacent carbon atom, increasing the electron density on the carbon atom, and making it more electron-rich.[27] This

property makes NHCs strong σ-donors in coordination chemistry.[28] It is important to note that, although stable and amenable to isolation and characterization, most free NHCs are still air- and moisture sensitive species and require handling under an inert atmosphere.[28]

# 1.4   Structure and properties of NHCs

The widespread use of NHCs as ancillary ligands for homogeneous catalysis is attributed not only to their peculiar electronic properties, but also to their ease of preparation and modification.[29] [30] Throughout the years numerous synthetic strategies have been developed, allowing for rapid diversification of NHC structures by simple variations in the starting materials.
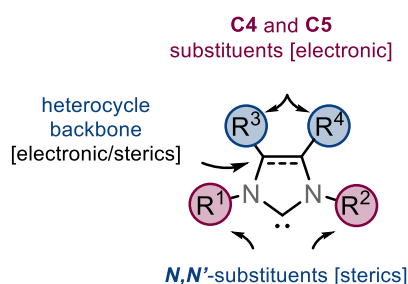


*Figure 9: Structural elements used to tune the stereo-electronic properties of classical imidazole in NHC ligands.*

This facilitates the modification of the steric and electronic properties of the resulting carbene ligand, thereby enabling synthetic chemist to experimentally explore the structure-activity relationship (SAR) between the ligand structure and the reactivity of the transition metal-catalyst.[30]  In the case of classical imidazol(in)-2-ylidene NHCs, electronic properties are mainly governed by the type of heterocycle and by the substitution pattern of the ring backbone (i.e. C4 and C5 positions), while steric properties are principally modulated by the nitrogen substituents (Figure 9). As a result of this diversification possibility, a myriad of NHCs with distinctive stereo-electronic features are now available, some of them are reported in Figure 10.[31]
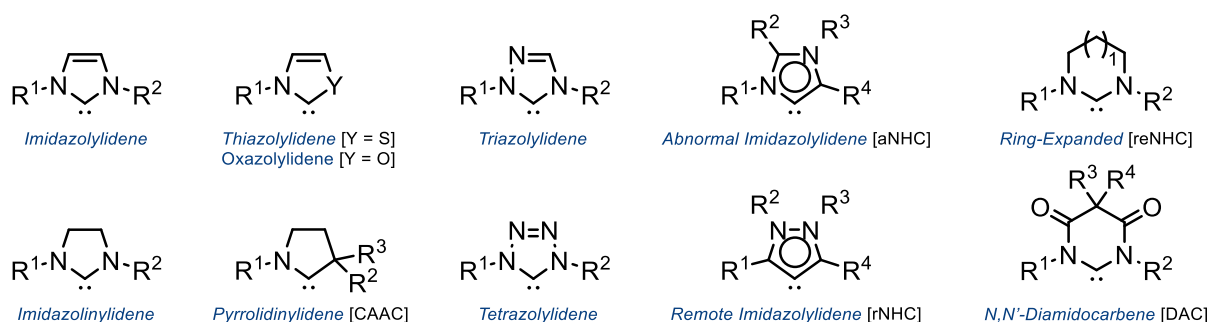
*Figure 10: Structures of some of the most applied classes of NHCs.*

Additional structural variability is obtainable by changing the *N*-substituents: they can impose additional steric properties on the bonded metal and can contain more hetero-atoms to form a multidentate ligand or even another carbene, in this case they are defined as multi-carbene ligands (Figure 11).[32]
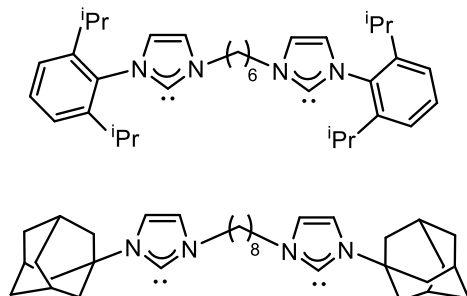


*Figure 11: multi-carbene NHC.*

In order to facilitate the decision-making among chemists when selecting or synthesizing appropriate NHCs for specific application, the use of a series of ligand descriptors becomes highly beneficial.[33] These descriptors have been developed, on the basis of experiments and calculations, to establish a quantitative relationship between specific structural features of a NHC and its electronic and steric properties. The steric characteristics of ligands have major implications on the reactivity of their respective complexes, often prevaricating their electronic influences.[34] However, when it comes to

NHC ligands, only a small number of these descriptors are commonly available and/or have been specifically developed for them.

## 1.5  Steric parameters

The most often applied steric parameter in organometallic chemistry was developed by Chadwick Tolman in 1977, primarily for phosphine ligands (Figure 12).[35] The so-called Tolman cone angle was originally determined from simple 3D space filling models, where the distance between the metal and the phosphine ($d$) was calibrate to 2.28 Å. [36]
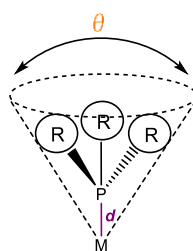


*Figure 12: Tolman cone angle ϑ for symmetrical phosphines.*

Looking at the Figure 13, the R-substituents of phosphines normally point away from the metal center. The cone angle θ (theta) indicates the approximate amount of "space" that the respective ligand occupies.[27] The bigger R-groups of a bulkier phosphine would be more spread-out giving rise to a larger cone and a bigger θ value. However, the use of the angle θ is limited to ligands, which bind to the metal in cone shape manner.[35] In fact, it is less suited for NHCs which do not coordinate to metal centers in a cone-shape manner. Indeed, NHCs exhibit a sort of "umbrella" shape geometry around the metal center, with steric impacts that is, generally, unevenly distributed.[37] Furthermore, many NHCs possess structural flexibility and, therefore, the ability to adapt their conformation in response to different coordination environment around the metal center.
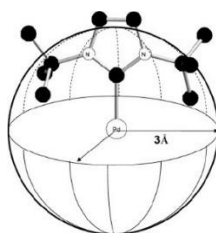
*Figure 13: Buried Volume (%Vbur).[38]*

To obviate to these shortcomings, Nolan, Cavallo and co-workers developed the concept of percent buried volume (%Vbur)[39] and steric maps (Figure 13).[40] The percent buried volume (%Vbur) is defined as the percentage of the total volume occupied by the ligand within an imaginary hemisphere with a defined radius of 3.5 Å, with the metal atom situated at the center of this hemisphere. The determination of %Vbur can be achieved either experimentally (i.e., single-crystal X-ray diffraction analysis) or using computational methods. The information provided by %Vbur is effectively complemented by steric maps, which provide a visual representation of the ligand's spatial distribution through a color-coded contour plot depicting different levels of steric hindrance around the metal center (Figure 14).
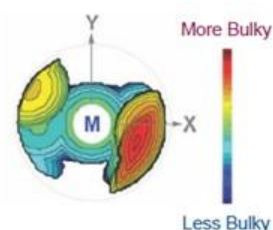


*Figure 14: Steric Map.[41]*

Unlike the Tolman cone angle, which focuses on specific characteristics of certain ligand class (i.e., phosphines), the %Vbur and Steric Maps provide insights into the spatial occupation around the metal center regardless of the type of ligand considered, thereby allowing for the establishment of property-structure relationships for a wide range of catalysts and ligands. In the case of NHCs, the percent buried volume is influenced by various factors, including the nature of the ligand's backbone, N-substituents, and the size of the ligand's ring.[41]

# 1.6 Electronic parameters

One of the oldest descriptors developed to quantify the electronic properties of a ligand is the Tolman electronic parameter (TEP). The purpose of the TEP is to understand deeply the σ-donation properties of two-donor-ligands (**L**) using Infrared Spectroscopy. [35]
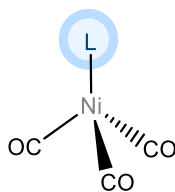


*Figure 15a: Model compound for TEP.*

[LNi(CO)$_3$] were chosen as model compounds because they can be readily prepared from tetracarbonylnickel(0). This kind of complexes are generally obtained by exposing ligand L to a solution of [Ni(CO)$_4$] in CH$_2$Cl$_2$ and subsequently subjecting them to infrared measurements (Figure 15a). TEP is based on the observation of the IR position of the CO stretching: a strong σ-donor ligand would make the complex more electron-rich, resulting in an increased amount of π*- backdonation to CO and further weakening of the CO bond. This would be reflected by the bathochromic shift of the monitored CO stretching frequency ($v$(CO)): the position shift of a signal to longer wavelength (lower energy).[42] Contrarily, a nickel complex with a weak σ-donor would be less electron-rich, resulting in the hypsochromic shift of the monitored CO stretching frequency: the shift of the signal goes to shorter wavelength (higher energy). Initially developed for tertiary phosphines and phosphites, the application of TEP to NHC ligands poses challenges, particularly for NHC ligands bearing particularly bulky N-substituents.[43] [44] Notably, the use of the bulkiest NHCs, in an exchange reaction with [Ni(CO)$_4$] resulted in the formation of highly unusual three-coordinate [(NHC)Ni(CO)$_2$] complexes,[44] making TEP determination problematic for this class of ligands to overcome these problems and to avoid the use of toxic [Ni(CO)$_4$], alternative carbonyl systems have been developed based on Rh(I) and Ir(I) (Figure 15b).
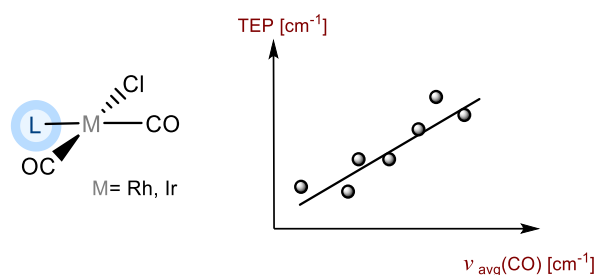
*Figure 15b: alternative carbonyl systems based on Rh(I) and Ir(I) to quantify electronic properties using IR spectroscopy.*

The approach is originated from Crabtree's observation that between the average infrared stretching frequency ($\nu$avg(CO)) of the cis-[Ir(L)(CO)$_2$(Cl)] systems and the A1 stretch in [(L)Ni(CO)$_3$] complexes, a linear correlation could be established for a series of ligands where data were available for both systems.[45] As such, it became practical to evaluate the Tolman electronic parameter of bulkier NHCs through extrapolation/interpolation. Despite obtaining a robust linear correlation (R2 = 0.91), the main criticism to Crabtree's system arose from the inconsistent collection of IR data for Ir(I)- and Ni(0)-systems, particularly relating to the solvent used during spectral recording. Although Nolan and co-workers addressed this issue by systematically recording IR data using a larger set of NHC ligands, all collected under the same conditions (which in turn led to an improved linear correlation of $R^2$ = 0.97),[46] it was through the work of Wolf, Plenio and their colleagues and the concomitant accumulation of IR data on *cis*-[Rh(L)(CO)$_2$(Cl)] complexes in the literature that a solid relationship between Rh(I), Ir(I),[47] and TEP was established.[31] Presently, these *cis*-[M(L)(CO)$_2$(Cl)] carbonyl systems (with M = Rh, Ir) serve as the predominant platform for determining the electronic properties of nearly every newly synthesized NHC ligand. The steric bulk of the ligand also plays a crucial role in modulating the reactivity and stability of metal complexes, therefore over the course of the year various molecular descriptors have been developed to assess the spatial requirements of a ligand from the perspective of the metal center.

# 1.7 Synthetic Access to Late Transition Metal-NHC Complexes

The incorporation of *N*-heterocyclic carbene ligands in metal complexes has significantly expanded the repertoire of homogeneous catalytic processes,[48] enabling the synthesis of valuable compounds with enhanced efficiency and reduced environmental footprint. However, limitations in the synthetic accessibility of any homogeneous (pre)catalysts constitutes a significant hinderance in their development and widespread application. Hence, the provision of facile, dependable, and efficient synthetic methodologies for this class of compounds always assumes paramount importance. In the case of late transition metal-NHC complexes, the advent of the first "bottleable carbene" by Arduengo and co-workers in 1991,[11] and their subsequent recognition as highly effective pre-catalysts for a wide range of chemical transformations, has served as a pivotal impetus for the advancement and progress in the synthesis of this class of compounds, reflecting the imperative need to address any synthetic bottleneck effectively. Consequently, contemporary synthetic chemists are now equipped with a series of different strategies to access these valuable organometallic compounds,[49] the most common of which can be broadly categorized as occurring through: **1**) the free carbene route; **2**) the built-in base route; **3**) the transmetallation route; **4**) the weak-base route (Scheme 1).

## 1.7.1 The Free Carbene Route

The most straightforward approach to affix an NHC ligand to a metal center involves the direct reaction of a free NHC, either isolated or generated *in-situ* (Scheme 1a), with the desired metal precursor in a ligand displacement reaction, or alternatively by cleavage of coordinatively unsaturated dimeric metal complexes, where the enthalpically favorable bridge-cleavage results in the formation of a coordinatively saturated metal centers. The synthesis of a free NHC encompasses a variety of methods,[18] the choice of which is predominantly influenced by the specific combination of NHC, and metal precursors utilized, but one of the most commonly encountered methodologies to generate a free NHC involves a typical Bronsted-Lowry acid-base reaction between an azolium salt and a strong base (such as NaH, KO*t*Bu, KHMDS, or *n*-BuLi) in an aprotic solvent. In line with typical Bronsted-

Lowry acid-base reactions, the resulting free NHC itself displays strong basicity/nucleophilicity, and, although the "*push-and-pull effect*" provided by the adjacent N-atoms provides enough stabilization as to allow their isolation, their handling and isolation usually require strictly anhydrous conditions and the use of degassed solvents.[48]

## *1.7.2 The Built-In Base Route*

An alternative method that circumvents the need for expensive, pyrophoric and strong bases is the "built-in base" approach (Scheme 1b). In this strategy, an azolium salt is subjected to treatment, under (generally) aerobic conditions and in environmentally friendly solvents, with suitable metal precursors, such as Pd(acac)$_2$,[103] Cu$_2$O,[104] or Ag$_2$O,[105] all of which already contain an embedded base. This reaction yields the desired carbene-metal complex and a protonated moiety as the sole by-product. Although the built-in approach is generally effective, however, its scope is somewhat limited those metal precursors that already possess a labile basic moiety. Incorporating this moiety into other metal precursors of interest can be challenging and presents a non-trivial synthetic problem, making this method less straightforward in certain cases. Nonetheless, the built-in base approach represents a valuable alternative in the organometallic synthesis of transition metal-NHC complexes.

## *1.7.3 Transmetallation Route*

Certain metal-NHC complexes can be obtained through a transmetallation process, where the NHC moiety is transferred from a pre-formed transition metal-NHC complex to another metal center (Scheme 1c). The most notable approach involves the use of Ag-NHC complexes as carbene transfer agents, which was first reported by Lin and colleagues in 1998.[50] Despite its widespread application, the transfer of NHC from silver does not always proceed smoothly, and the high cost and light-sensitivity of silver compounds have motivated researchers to seek alternative transmetalating agents. In this regard, Cazin and co-workers proposed, the utilization of Cu(I) carbene derivatives as less expensive and almost equally effective agents for preparing a diverse range of complexes with various transition metals,[51] such as Au, Ru, Ir, Rh, and Pd.

## 1.7.4  The Weak-Base Route

Popularized by Nolan[110] and Gimeno[52] in 2013, the "weak-base" route represents a more contemporary approach to synthesizing transition metal-NHC complexes (Scheme 1d.).[53] This method entails treating an azolium salt under aerobic conditions with a cost-effective, environmentally friendly base, such as NaOAc, $K_2CO_3$, $NEt_3$, or $KHPO_3$, in presence of the metal precursor of interest. Notably, these reactions are conducted using green solvents such as acetone, ethanol, or ethyl acetate, with (generally) moderate heating require to ensure reasonable reaction times. Another notable advantage of this approach is its broad applicability to a diverse range of structurally varied NHC ligands and transition metal precursors, rendering it a dependable and versatile method to access this class of compounds.
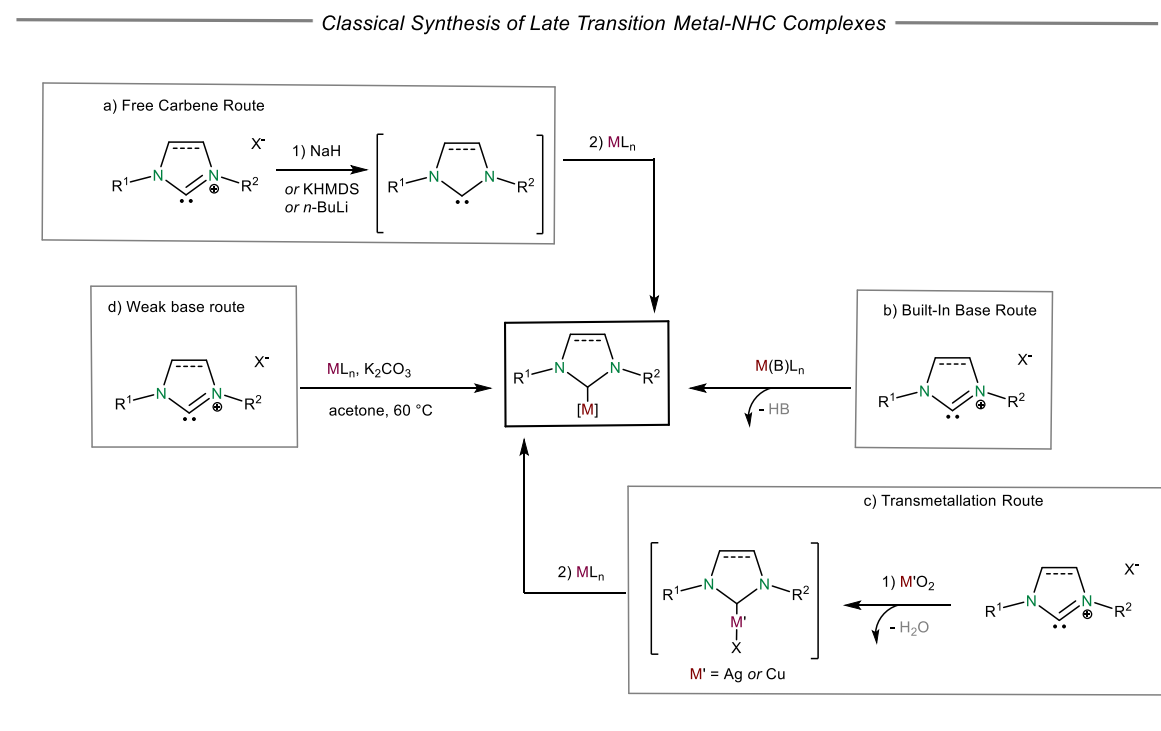


*Scheme 1: Common synthetic strategies for the assembly of late transition metal complexes bearing NHC ligands.*

# Chapter 2

## *Hydrosilylation of alkenes and alkynes with Pt-based catalysts*

## 1.1   Introduction

Hydrosilylation is the addition of silicon-hydrogen bonds across unsaturated carbon-carbon bonds. This reaction is highly sustainable, not only because it utilizes reagents which are inexpensive, stable, and earth abundant, but also since it is fully atom economical,[54] the reaction can be carried out under solvent-free and mild conditions.[55] The hydrosilylation, that has been proven to be one of the most efficient reactions in the silicone industry, is not only used on the laboratory scale but have been also implemented in the chemical industry. Theoretically, hydrosilylations are 100% atomic economic without generating other products or wastes.[56] Thus, apart from their importance for applications in the silicone industry, hydrosilylation is increasingly attractive for basic materials science. There is a lot of commercially significant hydrosilylation reactions: for example, the production of the siloxane derived from 1-octene and bis (trimethylsilyloxy) methylsilane  (MD'M) is on a large scale (~6,000 ton/year) and is employed to make weatherproof masonry products, metal oxides, and glass.[57] The considerable number of organosilicon compounds used in our daily lives means that a necessary challenge is to develop greener organosilicon chemistry.[58] In general, organosilicon compounds are characterized by stable and inert carbon–silicon bonds; compared to their ordinary pure carbon analogues, organosilicons have complementary physical properties, which make them attractive for a variety of industrial applications.[59] Hence, organosilicon compounds are widely found in adhesives and coatings and used as oils, rubbers, grafting agents and resins.[20] Alkyl, alkenyl, and aryl silicon derivatives are important in organic synthesis as surrogates for their boron and tin counterparts.[54] Silicon derivatives are often innocuous, stable, and cheaper than their related organometalloids. Therefore, there has been a great impetus to assemble organosilanes in a rapid, selective, and atom-economical way.[60] In this regard, hydrosilylation is the reaction that best meets all these requirements.[56]

The Hydrosilylation of alkenes (Equation 1, Scheme 2) and alkynes (Equation 2, Scheme 2), by the addition of a silicon-hydrogen bond across the C-C π-bond, forms a new (terminal) alkylsilane or vinylsilane. The Hydrosilylation of alkynes can yield three regioisomers: the $\alpha$, the $\beta$-($E$), and the $\beta$-($Z$) isomers. Their ratio depends on the alkyne, the ligands, the metal center, and the silane employed. This particular selectivity has been studied extensively, and only few catalytic systems have enabled the selective synthesis of each regioisomer.[60]



eq.1

eq.2
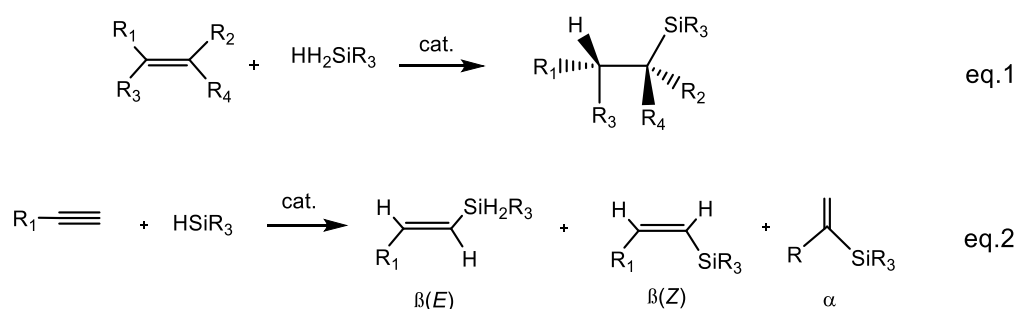
*Scheme 2: General hydrosilylation reaction of alkenes and alkynes.*

## 1.2 Platinum complexes with carbenes used in the reaction

Although thermodynamically favored, hydrosilylation must be catalyzed so as to be operative, it has been catalyzed by disparate complexes with many different metals, those based on homogeneous noble metals such as platinum, rhodium, and palladium are the most commonly used.[54] Platinum-catalyzed hydrosilylation of alkenes and alkynes is one of the most powerful methods of producing a variety of organosilicon compounds on both laboratory and industrial scales.[54] Several platinum compounds are easily available from commercial sources, and reactions rapidly proceed with only a small amount of the catalyst, being highly tolerant to various functional groups.[61] Although excellent activity and selectivity can be obtained, the price, purification, and metal residues of these precious catalysts are problems in the silicone industry.[62] Since the first hydrosilylation reaction ap-

19

peared in the academic literature in 1947, platinum-based catalysts dominated this area.[63] Originally, the introduction of Speier's catalyst ($H_2PtCl_6$) was a breakthrough.[58] Later on, Karstedt made an important contribution to this area by developing a Pt(0) complex containing vinyl-siloxane ligands.[64] Despite the efficiency of this system, there are indisputable drawbacks of homogeneous Pt-based catalysts. For instance, platinum is easily trapped in the product, which is viscous, making it difficult to remove it. However, the residual platinum can be separated from many hydrosilylation products, like volatile and soluble organosilanes, by using membrane-assisted nanofiltration or by simple distillation of the product.[59] Thus, the use of platinum for such processes is still justified, since the activity and selectivity are more relevant than the cost of the catalyst, which can, after all, be recycled.[55] From an industrial point of view, the high price of platinum (it was estimated that consumption of platinum accounts for up to 30 % of the cost of silicones) strongly motivates researchers to replace platinum with other recyclable, more earth-abundant and less expensive catalysts namely iron, nickel, and cobalt.[57] Since the pioneering discovery of Speier et al. in 1957, platinum became the workhorse of hydrosilylation due to its superlative ability to insert into the very strong silicon-hydrogen bond (75–100 kcal/mol) and produce relatively stable silyl platinum hydride complexes.[17] A significant progress was made in 1973, when Karstedt described a platinum catalyst obtained by the reaction of hexachloroplatinic acid with 1,3-divinyltetramethyldisiloxane (dvtms) ( Figure 16) .[65] Despite its structure was only solved several years later, the new complex gradually supplanted Speier's catalyst in industrial and academic applications due to its shorter induction period and enhanced activity. Still today, it is commonly used and serves as a standard for any new catalyst in the hydrosilylation of olefins.[66] Despite this success, different drawbacks persist: it lacks adequate selectivity, there is the formation of substantial quantities of undesired side-products, especially isomerized and reduced alkenes.[67] Moreover, the low stability of this Pt(0) complex leads to its degradation into platinum colloidal species, manifested by the appearance of a yellow to dark brown color in the reaction mixture. [68] Recently, Markó and co-workers achieved excellent results by with Pt(0)-*N*-heterocyclic carbene complexes as pre-catalysts (Figure 16).[55] Compared to Karstedt's complex, maybe the major steric protection around the Markó catalyst is the reason of its better selectivity, enhancing the addition of platinum to the less hindered side of the olefin. It is noteworthy that these catalysts exhibit a high stability under the reaction conditions, due to the

strength of the NHC-Pt bond, and no platinum colloids are formed during the benchmark hydrosilylation reactions.[55]
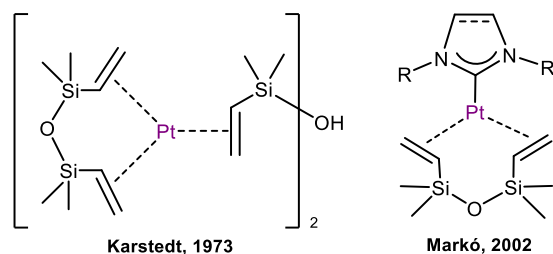


Figure 16: structure of the Karstedt's and Markó's catalysts.

Each of these three catalysts is platinum-based, in fact, notably, platinum-catalyzed hydrosilylation reactions of alkenes and alkynes stand out as a potent method for generating a diverse array of organosilicon compounds, applicable both in laboratory and industrial settings.[69] Several commercially available platinum compounds facilitate reactions that proceed rapidly with only a minimal amount of catalyst, displaying high tolerance to various functional groups.[54] Each year, a substantial quantity of platinum is utilized by the silicone industry, significantly impacting the pricing of silicone products.[55] Specifically, in the mentioned applications, the physical characteristics such as morphology and viscosity of the resulting product hinder the practical recovery of the Pt-based catalyst. Consequently, the catalyst is considered as a consumable rather than a reusable component. In 2007, approximately 5.6 metric tons of platinum were utilized by the silicone industry for this purpose.[57] Recent research efforts have been directed towards substituting platinum with alternative transition metals abundant in the Earth's crust and more economically viable, such as iron, nickel, and cobalt.[70] However, in the case of many hydrosilylation products, such as volatile and soluble organosilanes, the residual platinum can be recovered through straightforward techniques like product distillation or alternative methods like membrane-assisted nanofiltration.[71] Consequently, the utilization of platinum in these processes remains justified, as the paramount factors of activity and selectivity outweigh the economic considerations of the catalyst. Moreover, within certain chemical applica-

tions, particularly in the realm of silicone release coatings and rubber production, the catalytic properties related to specific chemical transformations (chemoselectivity) and preferred reaction sites (regioselectivity) hold greater significance than the economic cost of the catalyst itself.[66]

Despite numerous publications and patents highlighting the success of platinum-catalyzed hydrosilylation in the context of carbon-carbon multiple bonds, there is a surprisingly limited number of contributions dealing with the hydrosilylation of carbon-oxygen double bonds using platinum-based precatalysts.[69]

# 1.3   Mechanism of hydrosilylation

The hydrosilylation of alkenes, alkynes and similar compounds is important in synthetic chemistry because organosilicon compounds serve as valuable intermediates in organic synthesis; consequently, extensive research has been conducted on hydrosilylation, with considerable efforts directed at understanding its reaction mechanism. Two very similar reaction mechanisms have been identified during which the only difference lies in the position in which the migratory insertion occurs.

## 1.3.1   Chalk Harrod and modified Chalk Harrod mechanism of hydrosilylation

The hydrosilylation of terminal alkenes by silanes catalyzed by *N*-heterocyclic carbene platinum(0) complexes has been investigated.[60] Platinum catalysts, including both Speier's catalyst and Karstedt's catalyst, are believed to follow the Chalk-Harrod mechanism. The mechanism involves oxidative addition of silane to a Pt(0) complex, migratory insertion of an olefin into the metal-hydride bond, and reductive elimination to form the silicon-carbon bond in the organosilane product.[72] More recently, a related but different mechanism, often called the modified Chalk-Harrod has been recognized, and it involves insertion of the olefin into the silyl group instead of the metal-hydride bond (Figure 17).
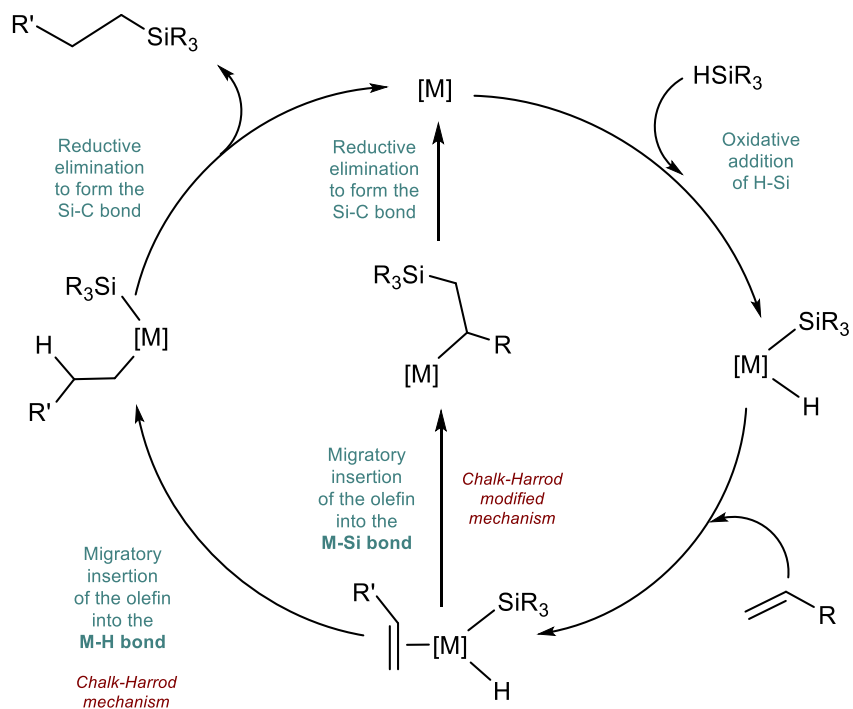
*Figure 17: Chalk-Harrod mechanism and Chalk-Harrod modified mechanism.*

# Chapter 3

*Experimental part*

## 1.1   Introduction

This project stems from the already initiated work on Pt-thioether catalysts tested for the first time directly in the hydrosilylation reaction by the Nolan's research team at Gent University. Simple Pt(II)-thioether worked just as well as state-of-the-art platinum pre-catalysts, but their use has several considerable practical advantages.[73] These easily accessible Pt(II) compounds have been known for almost a century, and have been used as precursors for the synthesis of other pre-catalysts for hydrosilylation, however, as far as we know, their catalytic activity in this reaction has never been studied. One of the major advantages of these complexes is the simplicity of their synthesis, reported in the next paragraph. Both Pt(II)-thioether complexes can be obtained as mixtures of cis/trans isomers in quantitative yields, simply by reacting $PtCl_2$ with the corresponding sulphide in $CH_2Cl_2$. Alternatively, $K_2PtCl_4$ can be used as a platinum precursor instead of $PtCl_2$.[73]

# 1.2 Catalysts synthesis

## 1.2.1 Synthesis of [Pt(DMS)$_2$Cl$_2$]

In a 1000 mL round-bottom flask, a solution of K$_2$PtCl$_4$ (15.500 g, 37.34 mmol, 1.00 equiv.) in demineralized water (600 mL) was introduced and placed in an ice bath. DMS (15.50 mL, 209.56 mmol, 5.61 equiv.) was then added with vigorous stirring, leading to the rapid formation of a pale pink precipitate (a Magnus-type complex with the formula [Pt(DMS)$_4$][PtCl$_4$]). Subsequently, the flask was equipped with a reflux condenser, and the resulting mixture was heated to 80 °C and stirred at this temperature for 10 minutes until the solution turned clear yellow. Following this, the mixture was cooled to room temperature and extracted with CH$_2$Cl$_2$ (4x200 mL) until the solution became colorless. The combined organic fractions were then dried over anhydrous MgSO$_4$ and evaporated to dryness, yielding the desired complex **6** as a yellow crystalline solid (14.570 g, >99% yield).
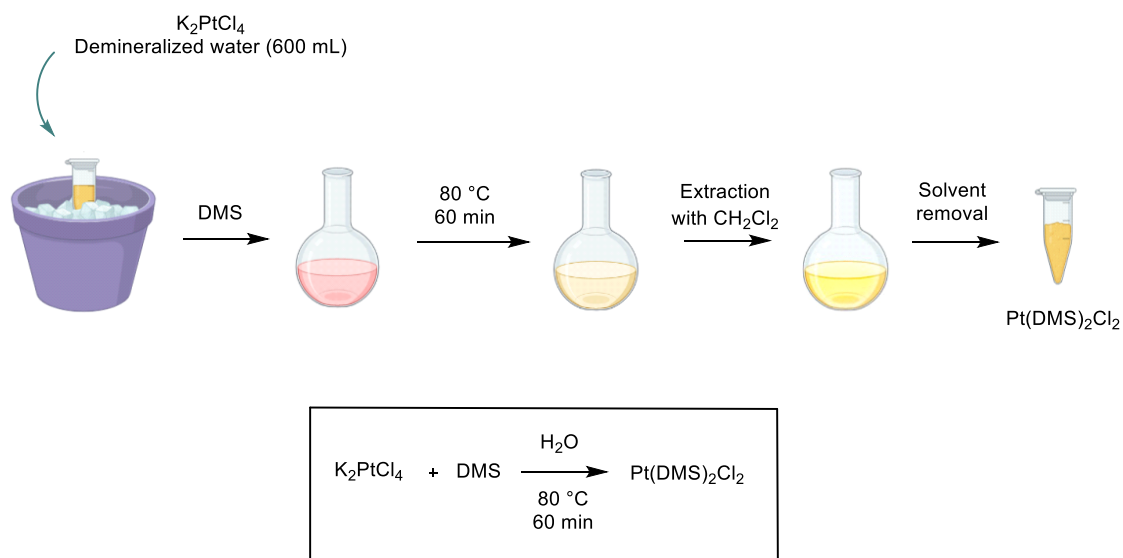


*Scheme 3: synthesis of [Pt(DMS)$_2$Cl$_2$] from K$_2$PtCl$_4$.*

## 1.2.2 Synthesis of [Pt(THT)$_2$Cl$_2$]

A 20.0 mL vial was loaded with PtCl$_2$ (250.0 mg, 0.940 mmol, 1.0 equiv.) and CH$_2$Cl$_2$ (5.0 mL). THT (THT = tetrahydrothiophene) (500 µL, 5.671 mmol, 6.0 equiv.) was then introduced, and the vial was securely sealed with a septum screw cap. The resulting mixture underwent stirring at 20 °C for 60 minutes. Following this duration, a complete disappearance of the dark PtCl$_2$ was noted, resulting in the formation of a clear orange solution. The volatile components were subsequently evaporated under vacuum, yielding the desired complex **1** as an orange powder (414.0 mg, >99% yield). Both Pt(II)–thioether precatalysts **1-6** can be easily synthesized through the reaction of PtCl$_2$ with the respective sulfide in CH$_2$Cl$_2$ as shown in Scheme 4.
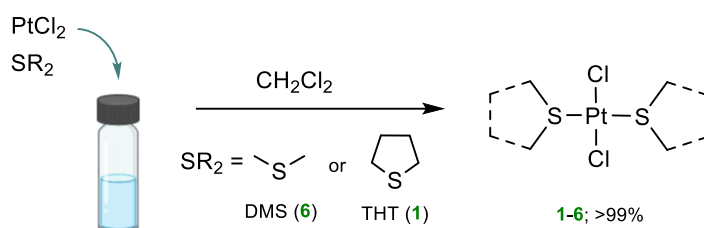


Scheme 4: Synthesis of Pt(II)-thioether complexes **1** and **6**.

Four other catalysts based on carbene systems were also used in this thesis project in addition to the two described above and are all shown in Figure 18. Recently outstanding results were achieved by Marko and co-workers with Pt(0)-*N*-heterocyclic carbene complexes as pre-catalysts. Compared to Karstedt's complex, the Pt(0)-NHC complexes were shown to be much more selective, presumably because of the increased steric protection around the platinum atom, enhancing the addition of platinum to the less hindered side of the olefin. What is equally important, due to the strength of the NHC-Pt bond, is that this new generation of catalysts is remarkably stable under the reaction conditions and no formation of platinum colloids was observed during the benchmark hydrosilylation reactions. We try to explore the catalytic activity of a recently disclosed family of easily accessible well-defined Pt(II)-NHC pre-catalysts.[55] In the course of recent studies, it was developed a

sustainable and facile synthetic route to Pt(II)-NHC complexes. The operationally simple protocol, involving a weak-base-mediated reaction between platinum precursors and azolium salts under mild and open-to-air conditions, allowed us to obtain a series of air- and moisture-stable complexes of general formula [Pt(NHC)(L)Cl$_2$].
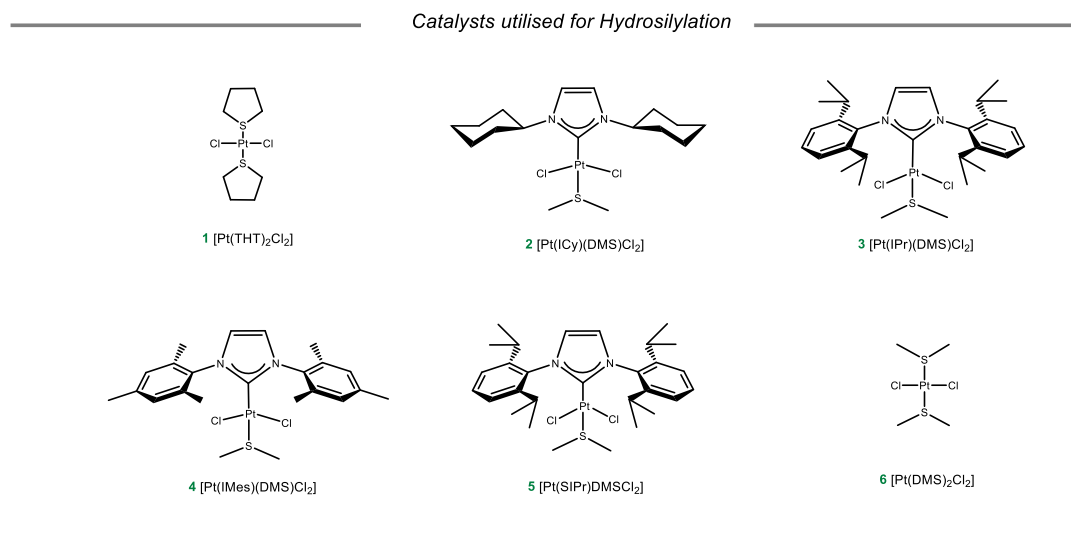


*Figure 18: Catalysts structures utilized in this project.*

# 1.3 Alkenes hydrosilylation

The reaction of hydrosilylation was tested both on alkenes and alkynes substrates. The investigation started by comparing the activity and selectivity of [Pt(DMS)$_2$Cl$_2$] and [Pt(THT)$_2$Cl$_2$] on 1-octene. The general Scheme of the reaction is depicted in the Scheme 5.
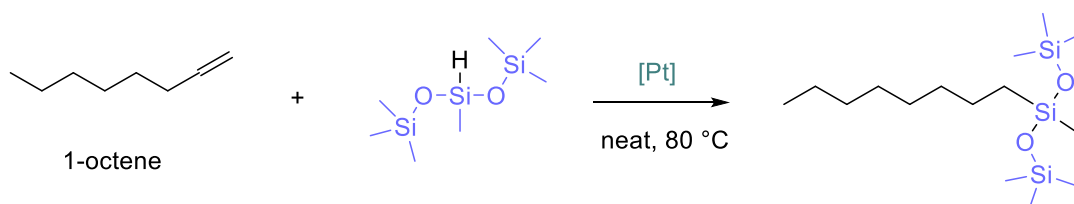


*Scheme 5: General hydrosilylation reaction of 1 octene.*

The reaction was conducted always at 80 °C and the difference lays on the type of catalyst utilized and the amount of it. In fact, it was tried to carry the reaction with 1000 ppm, 100 ppm, 10 ppm, 1 ppm and 0.1 ppm of catalyst. The smaller the amount of catalyst used, the longer the allowed reaction time. In fact, for 0.1 ppm and 1 ppm of catalyst, the yield was measured after 90 and 180 minutes. Next, reactions conducted with 10 ppm of catalyst were tested after 5, 15 and 60 minutes, the same for those with 100 ppm. Finally, for reactions conducted with 1000 ppm catalyst, the yield was measured only after 5 and 15 minutes.

# 1.4 Substrates scope

The hydrosilylation reaction was then tested on various alkene substrates to demonstrate that the conditions are optimal for substrates of different natures and properties. The products obtained with the corresponding yields are reported in Figure 19. As can be seen, the 1,7-octadiene (**1**), an aromatic substrate (**3**), an ether (**4**), and epoxide (**7**) substrates were tested. It was used also a different silane on one substrate: the 1,1,3,3, -tetramethyldisiloxane (**6**) but it worked worse than the MD'M usually used. All reactions exhibited high conversion (>90 %) after 24 hours except the one performed with TMDS instead of MD'M.
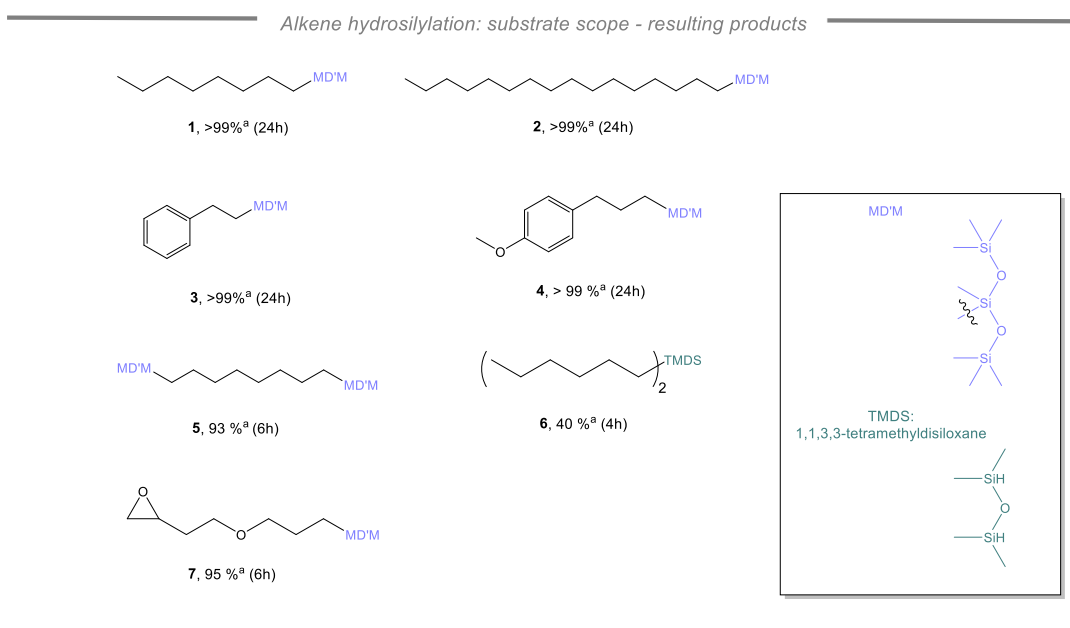


*Figure 19: resulting products from alkenes hydrosilylation.*

[a] Determined by ^{1}H-NMR (some representative spectra are reported in the appendix).

# 1.5 Results

*Table 1a: Optimization of the hydosilylation of 1-octene.*

| Entry | [Pt] catalyst | Cat. Loading [mol%] | T [°C] | Time [min] | Yield [%] [a] |
|:---:|:---:|:---:|:---:|:---:|:---:|
| 1 | [Pt(DMS)$_2$Cl$_2$] | 0.00001 | 80 | 90/180 | 50/60 |
| 2 | [Pt(THT)$_2$Cl$_2$] | 0.00001 | 80 | 90/180 | 46/56 |
| 3 | [Pt(DMS)$_2$Cl$_2$] | 0.0001 | 80 | 90/180 | **>99/>99** |
| 4 | [Pt(THT)$_2$Cl$_2$] | 0.0001 | 80 | 90/180 | 93/97 |
| 5 | [Pt(DMS)$_2$Cl$_2$] | 0.001 | 80 | 5/15/60 | 95[b]/96[b]/96[b] |
| 6 | [Pt(THT)$_2$Cl$_2$] | 0.001 | 80 | 5/15/60 | 95[b]/97[b]/ 97[b] |
| 7 | [Pt(DMS)$_2$Cl$_2$] | 0.01 | 80 | 5/15/60 | 89/90/90 |
| 8 | [Pt(THT)$_2$Cl$_2$] | 0.01 | 80 | 5/15/60 | 93/94/94 |
| 9 | [Pt(DMS)$_2$Cl$_2$] | 0.1 | 80 | 5/15 | **95/95** |
| 10 | [Pt(THT)$_2$Cl$_2$] | 0.1 | 80 | 5/15 | **96/96** |

[a] Determined by GC.

[b] Average of 3 runs.
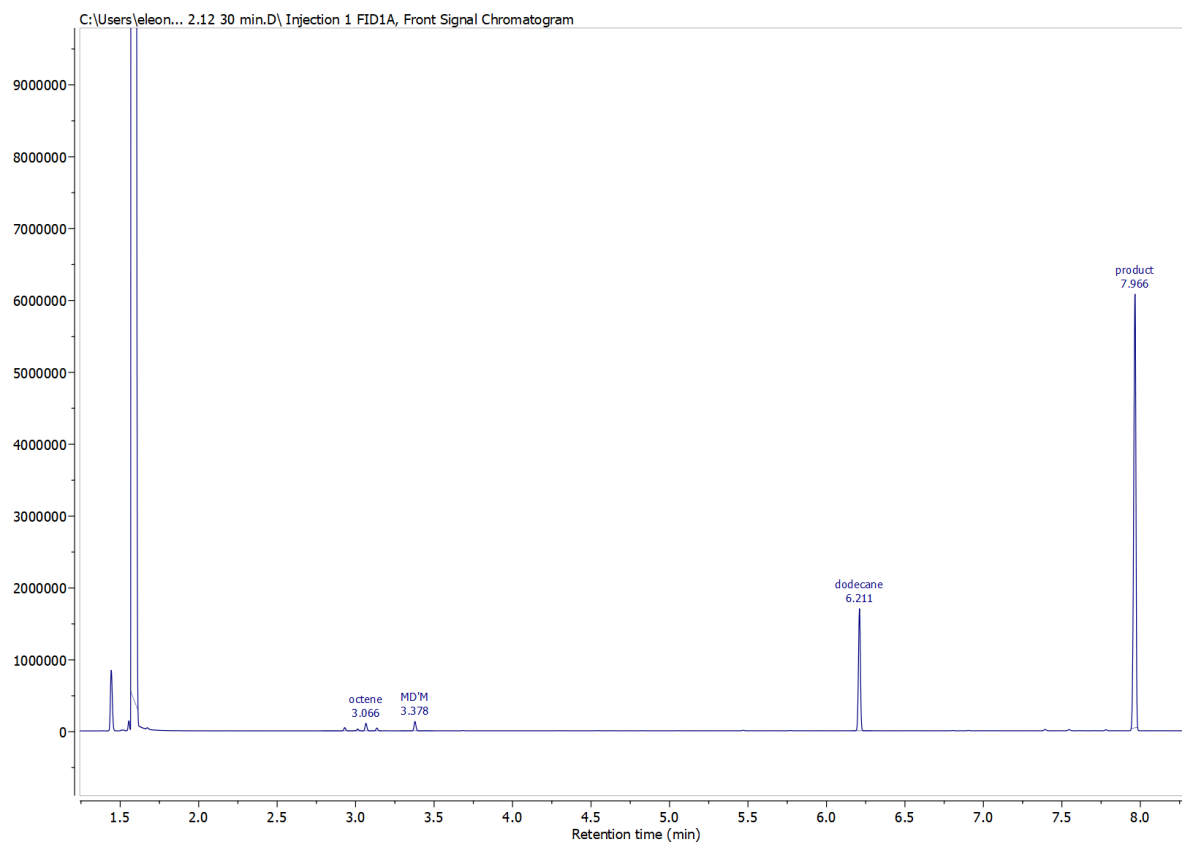
*Figure 20: GC spectrum of alkene-silane.*

In Figure 20 is reported one example of the GC spectrum obtained from the hydrosilylation of 1-octene. The first group of peaks at around 3 min is 1-octene and its isomers, the second peak at around 3.2 min is MD'M, then dodecane (used as internal standard) at 6.3 min and the product at 8 min.

with $[Pt(DMS)_2Cl_2]$ was obtained the best result: with only a catalyst amount of 1 ppm, a quantitative yield was obtained after 90 minutes (see entry 3 Table 1), and with the higher catalyst loading (0.1 mol%) already after five minutes the yield was 95% (see entry 9 Table 1). With the same catalyst loading values but using $[Pt(THT)_2Cl_2]$ catalyst, slightly lower yields were obtained: for catalyst loading at 1 ppm, a yield of 93 percent was obtained after 90 minutes and 97% after doubling the time (see entry 4 Table 1), while at a catalyst loading of 1000 ppm the yield after five minutes was 96% (see entry 10 Table 1).

32

# 1.6 Alkynes hydrosilylation

The reaction was conducted on two different alkynes, phenylacetylene and 1-octyne, with all the six catalysts shown in the Figure 18. The same amount of catalyst (0.1 mol%), was used in all cases. The general reactions schemes are reported in Scheme 6. The reactions were conducted with the substrate, the MD'M and the Pt-based catalyst (0.1 mol%) at 60 °C.
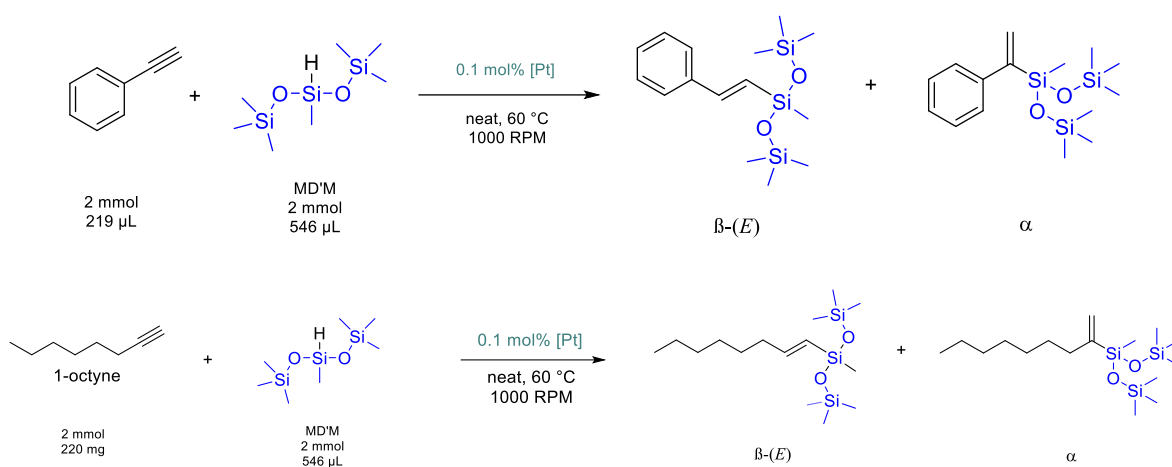


*Scheme 6: General reaction and conditions of the hydrosilylation of phenylacetylene and 1-octyne.*

# 1.7 HFIP: proprieties, use and acceleration of the re-action

In this study all the reactions were also performed using 1,1,1,3,3,3-Hexafluoroisopropanol (HFIP) and it was added in different amount (10 mol%, 20 mol% and 30 mol%). HFIP is a solvent that has garnered significant attention from the chemical community in recent years due to its recyclability and H-bonding donor properties in combination with its high acidity, cation-stabilizing ability and low nucleophilicity. [74] It is a polar solvent with strong hydrogen bond-donating properties, widely used in organic synthesis due to its ability to stabilize ionic species, transfer protons, and participate in various intermolecular interactions. Over the past decade, its use has grown, and recently, HFIP has also been explored as a ligand (in its alkoxide form) within metal coordination spheres, although only a few examples have been explicitly documented in the literature.[75] Analysis shows that it possesses a wide range of interesting and unique properties: it does not absorb UV light, is thermally stable and is miscible with both water and most common polar organic solvents.[75] The low boiling point enables easy recovery through distillation, resulting in reduced solvent waste and offsetting the initial cost (HFIP can be purchased at approximately UK£99/kg).[75] Industrial procedures for HFIP recovery on a large scale have been developed, involving co-distillation with heptanes and separation of the immiscible distillate. Therefore, HFIP has proven to be a uniquely simple tool rendering the need for external activators obsolete and leading to highly active catalytic systems with catalyst loadings as low as ppm levels in some cases.[76] HFIP can assume a dual role as a solvent and an activator in a lot of organic and inorganic catalysis. The use of HFIP has been reported in various reactions in organic chemistry[77] such as: in the activation of hydrogen peroxide to carry out epoxidation reactions of alkenes,[78] Baeyer-Villiger oxidation of ketones,[79] intramolecular Schmidt reaction,[80] Friedel-Crafts reaction of acyl chlorides,[81] and Hosomi-Sakurai allylation of dimethyl acetals[82]. In all of them, the hydrogen bond donating ability of HFIP allows the activation of the functional groups without the need to use catalysts or any additive.[83] In the case of our studies, hydrogen-bonding activation of Pt-Cl bonds was explored, following up on the unpublished results of the Nolan group showing promising potential of *in situ* generated cationic platinum complexes in alkyne hydrosilylation.

# 1.8  Results

All the results are reported in Table 1b and 1c, one for each substrate. Indeed, all reactions are found to be accelerated/activated to varying degrees when HFIP is added, with some results being more significant than others. Analyzing the results obtained with the phenylacetylene if we have a look to the entry 2 of Table 1a, the reaction using $[Pt(ICy)DMSCl_2]$ as the catalyst led to the highest conversion of the alkyne, second only to the reaction with $[Pt(DMS)_2Cl_2]$, which had the best conversion overall.  The reaction does not proceed after 4 hours without HFIP, however, with the addition of HFIP (10 mol%), after 1 hour a conversion of 25% is obtained and a complete conversion is achieved after 4 hours. It was also tried a higher amount of HFIP for the same reaction: 20 mol% and 30 mol% but anyway, the full conversion was achieved after 4 hours. An even better result can be seen with $[Pt(DMS)_2Cl_2]$  reported in entry 7 of the Table 1a: the reaction after 4 hours does not proceed, while the HFIP-assisted systems after the same time exhibit a complete conversion. Regarding 1-octyne, the most important results are shown in entries 1, 2, 3 and 6 of the Table 1c. The first one is the reaction with $[Pt(IPr*)DMSCl_2]$: without HFIP even after 23 hours the reaction does not proceed, however, with the addition of HFIP (10 mol%), the reaction is complete with a total conversion after just 4 hours. The reaction with $[Pt(ICy)DMSCl_2]$ shows no conversion after 4 hours under normal conditions but half full conversion with HFIP (10 mol%) and after 23 hours the conversion is total if HFIP is used. An improvement in reaction conversion with the addition of HFIP is also observed in the one shown in entry 3 of the Table 1c: with the $[Pt(SIPr)DMSCl_2]$ as catalyst the reaction does not proceed and only with HFIP a complete conversion can be achieved after 23 hours. The best result was obtained with the $[Pt(DMS)_2Cl_2]$ and HFIP (10 mol%), with a  full conversion after only 1 hour.

Table 1b: Results of hydrosilylation conducted on Phenylacetylene.

| Entry | Catalyst* | T (°C) | Conversion of Phenylacetylene (%) [b] | | | β-(E)/α[b] |
|---|---|---|---|---|---|---|
| | | | 1h | 4h | 23h | |
| 1 | [Pt(IPr*)DMSCl$_2$] | 60 | - / 0[c] | - / 0[c] | 0 / 0[c] | - / 0[c] |
| 2 | [Pt(ICy)DMSCl$_2$] | 60 | - / 25[c] / 34[d] / 37[e] | - / **>99**[c] / >99[d] / >99[e] | 12 / >99[c] | 0.51 / 0.89[c] |
| 3 | [Pt(ICy)DMSCl$_2$] [a] | 60 | 21[c] | 88[c] | >99[c] | 0.50[c] |
| 4 | [Pt(IPr)DMSCl$_2$] | 60 | - / 0[c] | - / 16[c] | 5 / 56[c] | 0.5 / 0.97[c] |
| 5 | [Pt(IMes)DMSCl$_2$] | 60 | - / 0[c] | - / 11[c] | 2 / 25[c] | 0.54 / 1.24[c] |
| 6 | [Pt(SIPr)DMSCl$_2$] | 60 | - / 10[c] | - / 33[c] | 4 / 87[c] | 0.5 / 0.94[c] |
| 7 | [Pt(DMS)$_2$Cl$_2$] | 60 | - / 92[c] | - / **>99**[c] | >99 | 0.73[c] |

*The catalyst loading is 0.1 mol %.

[a] A solution with the catalyst and DCM was prepared and used instead of the catalyst on its own, but it works worse than

the solid catalyst that is usually used.

[b] Determined by $^1$H NMR spectroscopy.

[c] Reaction with 10 mol% HFIP.

[d] Reaction with 20 mol% HFIP.

[e] Reaction with 30 mol% HFIP.

*Table 1c: results of hydrosilylation conducted on phenylacetylene.*

| | | | Conversion of 1-octyne (%) [b] | | | |
|---|---|---|---|---|---|---|
| Entry[a] | Catalyst* | T (°C) | 1h | 4h | 23h | β-(E)/α[b] |
| 1 | [Pt(IPr*)DMSCl$_2$] | 60 | - / 0[c] | - / **>99**[c] | 0 / >99[c] | - |
| 2 | [Pt(ICy)DMSCl$_2$] | 60 | - / 17[c] | - / 55[c] | 90 / **>99**[c] | 3.18 / 3[c] |
| 3 | [Pt(SIPr)DMSCl$_2$] | 60 | - / 0[c] | - / 27[c] | 29 / **>99**[c] | 3.65 / 3.5[c] |
| 4 | [Pt(IPr)DMSCl$_2$] | 60 | - / 0[c] | - / 20[c] | 18 / 78[c] | 2.3 / 2[c] |
| 5 | [Pt(IMes)DMSCl$_2$] | 60 | - / 0[c] | - / 27[c] | 29 / 79[c] | 1.2 / 0.9[c] |
| 6 | [Pt(DMS)$_2$Cl$_2$] | 60 | > **99**[c] | > 99[c] | - | 3[c] |

* The catalyst loading is always 0.1 mol %.

[a] Every entry is an average of 2 runs.

[b] Determined by $^1$H NMR spectroscopy.

[c] Reaction with 10 mol% HFIP after 4 h.

# *Conclusion Project 1*

The use of HFIP significantly increases the reaction efficiency. In the alkyne hydrosilylation, the best catalyst with and without addition of HFIP turned out to be the [Pt(DMS)$_2$Cl$_2$]. It is the only one that allows high conversions with added HFIP even after only 1 hour. For the reaction conducted on 1-octyne, the catalyst [Pt(IPr*)DMSCl$_2$] also performed well with a complete conversion after 4 hours, while it never showed any effectiveness with phenylacetylene, most likely because of the increased steric hindrance. For phenylacetylene, a good performance was achieved with [Pt(ICy)DMSCl$_2$], reaching full conversion after 4 hours, while the same catalyst used in the reaction with the other alkyl tested, required 23 hours to achieve the same result. In most reactions, that without HFIP do not proceed, when only 10 mol% of HFIP were added to the system, the conversion was as high as 99%. On the other hand, the selectivity of this transformation in the case of both phenylacetylene and 1-octyne turned out to be quite poor, compared to the state-of-the-art Pt(0)-NHC complexes, suggesting that HFIP contributes to catalyst decomposition.[84] In fact, in studies conducted on substrates identical to those used in this study (terminal alkynes), high selectivities towards the β isomer were achieved and the catalyst loading could be reduced to 0.01 mol% while still maintaining excellent selectivities. Details of the origin of the selectivity in favor of the β regioisomers remain unknown.[84]

<p style="text-align:center">**PROJECT 2**</p>

<p style="text-align:center">*Optimization of amide reduction with Sunthetics algorithm*</p>

# Chapter 1

## 1.1   Amines and their importance

Traditionally, amines have played a significant role in conventional remedies crafted from local herbs, which frequently contain alkaloids, a category of natural organic compounds containing nitrogen.[85] Moreover, the pharmaceutical and agrochemical industries feature a plethora of functionalized derivatives of amines, serving as prevalent active ingredients.[86] Amines are one of the most important functional groups in organic synthesis, particularly in scaffolds constituting the active ingredients of natural products, pharmaceutical molecules, and agrochemicals, they also play a crucial role in the production of bulk and fine chemicals, contributing to the manufacturing of plastics, textiles, surfactants, dyes, and various other products.[87] It is, thus, understandable that the development of new methodologies for the construction of complex amine architectures is an area of persistent interest in organic synthesis.

## 1.1.1   Synthesis of primary, secondary and tertiary amines historically

Although modern approaches have introduced fresh possibilities for amines synthesis, such as the $C(sp^3)$–H functionalization of amine derivatives[88] alternatively, the employment of photoredox chemistry to elaborate amine architectures through open-shell radical intermediates[89], substantial progress in enhancing the synthetic arsenal was achieved in the early decades of the 20th century, if not earlier: the Gabriel synthesis,[90] Schmidt reaction ,[91] the reduction of nitro (not only arenes)

<p style="text-align:center">40</p>

with a noble metal (Pd, Pt or Ni) in the presence of $H_2$ or with a metal (Fe, Sn or Zn) in the presence of an acid like HCl,[92] Staudinger reaction,[93] Hofmann rearrangement, reduction of nitriles[94] (e.g. with Lithium aluminum hydride ($LiAlH_4$)), are all of them routinely used to access primary amines (Scheme 1). The schematic representation of the Gabriel synthesis for primary amines and amino compounds can be summarized as in Scheme 1a: first there is the interaction between the conjugate base of phthalimide and an alkyl halide, resulting in the formation of an alkyl phthalimide. Potassium phthalimide is a -$NH_2$-synthon which allows the preparation of primary amines by reaction with alkyl halides. After alkylation, the phthalimide is not nucleophile and does not react anymore and the product is cleaved by reaction with base or hydrazine, which leads to a stable cyclic product. [95]

The significance of the Gabriel synthesis stems from:

- The availability of mild conditions for both stages.
- The prevention of secondary or tertiary amine by-products contamination in the primary amine.[95]
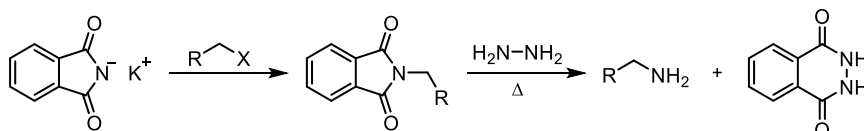- The ability to accommodate a broad array of other functional groups within the molecule. [96]

Thanks to its mild reaction conditions and high yields, it finds widespread use across various synthetic applications, making the synthesis particularly appealing. [95]

The Schmidt reaction (Scheme 1b) was initially a broad designation for a group of reactions in which hydrazoic acid was added to a carbonyl or another compound, leading to the insertion of a nitrogen atom into a chain or ring.[97] Within organic chemistry, the Schmidt reaction denotes an organic synthesis of primary amines, where an azide reacts with a carbonyl derivative, typically an aldehyde, ketone, or carboxylic acid, under acidic conditions, yielding an amine or amide while releasing nitrogen.[98] This intramolecular process has gained significance in natural product synthesis.[97] It proves effective in generating amines from carboxylic acids and amides from ketones. The prevalent variant involved the reaction with a carboxylic acid and the protonated azide undergoes the rearrangement.[91] In the Hofmann reaction, an amide undergoes conversion to an amine with one fewer carbon atom through treatment with bromine or chlorine and an alkali (Scheme 1d).[99] Essentially, this reaction eliminates the carbonyl group of the amide. It can be applied to produce amines from amides derived from aliphatic, aromatic, arylaliphatic, and heterocyclic acids.[100] Typically, the Hofmann
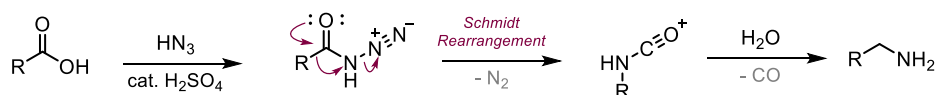
reaction is conducted by dissolving the amide in a slightly excess cold aqueous hypohalite solution, followed by rapid heating.[101]



*Scheme 1: some of the classical synthesis method of primary amines.*
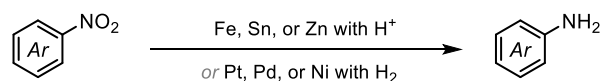
The catalytic hydrogenation of nitriles (Scheme 1e) is frequently the most cost-effective method for synthesizing primary amines. In the first phase of the reaction the nitrile reacts with the reducing agent to form an intermediate adduct.[102] For instance, in the presence of a strong reducing agent such as lithium aluminum hydride (LiAlH$_4$), a nitrile-aluminum adduct is formed. Then the carbon-nitrogen triple bond in the nitrile is reduced to a carbon-nitrogen single bond. This step can occur through various mechanisms, including nucleophilic attack of the reducing agent on the carbon of the cyano group.[103] The intermediate resulting from the reduction of the nitrile is then hydrolyzed, often with the addition of water or diluted acid, to yield the corresponding amine. Catalysts commonly used in this reaction include group 10 metals such as Raney nickel,[104] palladium black[105], or platinum dioxide.[106] In its traditional configuration, the Staudinger reaction (Scheme 1f) comprises two sequential stages: firstly, the electrophilic addition of an azide to the phosphorus center, resulting in the formation of phosphazide **1** and subsequently yielding iminophosphorane **2**.[107] Typically, the imination process occurs smoothly, with nearly quantitative conversion and minimal formation of by-products. [93] Afterwards, for the synthesis of secondary amines, there are the reductive amination,[108] the Mannich reaction, the Leuckart-Wallach reaction and the Delépine reaction,[109] all depicted in Scheme 2. All the primary or secondary amines that are obtained with these reactions can then be alkylated via reductive amination or direct N-alkylation to access tertiary amines.[69]Reductive amination, also referred to as reductive alkylation, is a pivotal method of amination that facilitates the transformation of a carbonyl group into an amine through an intermediate imine (Scheme 2a).[108] Typically, the carbonyl group involved is either a ketone or an aldehyde. This methodology stands as a prevalent approach for amine synthesis and is particularly valued in green chemistry due to its capacity for catalytic one-pot reactions under mild conditions. [110] The process unfolds through the interaction between a carbonyl compound and an amine in the presence of a reducing agent and it is conducted under neutral or weakly acidic conditions.[111] The Mannich reaction is widely employed in organic synthesis for the generation of secondary amines and other β-amino compounds, which serve as intermediates in diverse syntheses of pharmaceuticals, agrochemicals, and chemical materials.[112] In the reaction, first the carbonyl compound (ketone or aldehyde) reacts with the primary or secondary amine to form an imine or enamine intermediate and this step typically occurs under acidic conditions (Scheme 2b). Then the imine/enamine intermediate reacts with the compound containing an acidic hydrogen (e.g., formaldehyde or a derivative) through nucleophilic addition. This leads to the formation of a β-amino carbonyl compound. In certain instances, heating in the presence of a reductive agent like NaBH$_4$ is employed to yield the secondary amines.

**a**) Reductive Amination
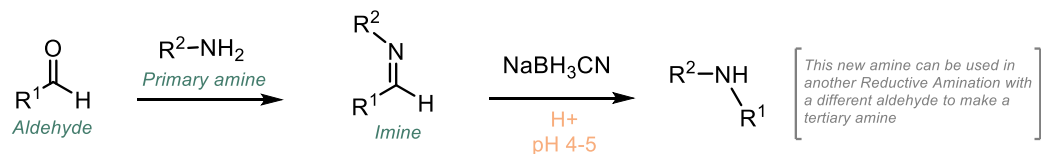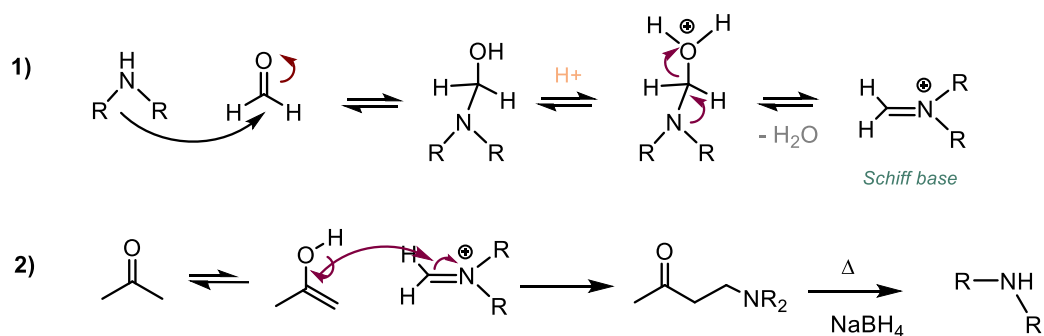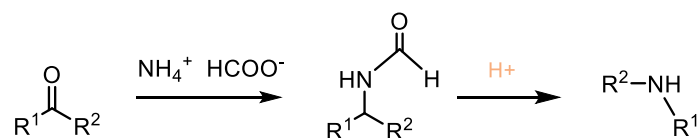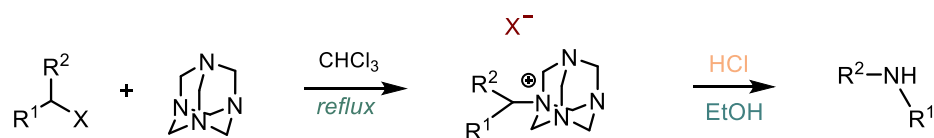


**b**) Mannich Reaction

**1)**



**2)**



**c**) Leuckart-Wallach Reactionh



**d**) Dèlepine Synthesis



*Scheme 2: Some of the classical synthesis methods of the secondary amines.*

One of the traditional techniques employed in the synthesis of secondary amines and derivatives is the Leuckart–Wallach reaction (Scheme 2c), involving the reductive amination of carbonyl compounds using a blend of formamide, formic acid, or ammonium formate.[113] The reaction represents a chemical transformation wherein aldehydes or ketones are converted into amines through reductive amination under elevated temperatures, typically ranging between 120 and 180 °C. Variations of this method utilize ammonium formate, formamide, or combinations of formamide and formic acid.[114] While it is a straightforward procedure, it presents several challenges such as the necessity for elevated temperatures and the simultaneous generation of N-formyl derivatives, which require subsequent acid hydrolysis. Consequently, the Leuckart–Wallach reaction proves unsuitable for thermally unstable and acid-sensitive molecules. A more efficient and high-yielding approach for the synthesis of racemic secondary and tertiary amines involves heating an aldehyde or ketone with cost-effective solid ammonium formate in refluxing toluene or benzene.[115]  One commonly employed method for synthesizing tertiary amines includes the reductive amination of carbonyl compounds (Scheme 4a) and the process involves multiple sequential steps. Initially, condensation between the carbonyl compound and the amine forms a carbinol-amine, which subsequently undergoes dehydration to yield either an imine or Schiff base. Following this, the imine intermediate is then reduced to form the amine.[116] A mixture of carbonyl compound and amine can commonly undergo reduction using formic acid (known as the Leuckart-Wallach reaction)[113] or specific metal hydrides.[110] Among these, sodium cyanoborohydride emerges as the most convenient reagent in the latter case.[117] Nevertheless, these approaches entail high costs and environmental concerns. A more pragmatic approach involves employing molecular hydrogen, alongside a supported or unsupported catalyst, as the reducing agent in this procedure.[116] Due to the highly reactive nature of these reaction intermediates, the conventional reductive amination of aldehydes and ketones occur as a series of successive and concurrent reactions, resulting in a mixture of primary, secondary, and tertiary amines and separating these reaction products can be challenging due to slight differences in their boiling points.[116] Hence, one of the critical concerns is controlling selectivity. While catalyst nature stands out as the most crucial factor in governing selectivity, it remains the least comprehended. Additionally, the substrate's structure and the employed reaction conditions can also influence selectivity to some extent.[116]

Subsequently, the Buchwald-Hartwig reaction follows, which is an important synthesis reaction for aromatic tertiary amines (Scheme 4b). Aromatic amines hold pivotal roles as essential products and foundational components in chemistry, particularly within the pharmaceutical and agrochemical sectors.[118] Traditionally, their synthesis relied on various methods, including nitration followed by reduction, nucleophilic aromatic substitution of activated substrates, or copper-mediated Ullmann-type coupling between amines and aryl halides (Scheme 3).[119] Despite their utility, these approaches exhibit restricted scope and limited tolerance towards functional groups. Nitration, although an established and cost-effective technique, suffers from inefficiencies in overall step economy during aromatic amine synthesis. The emergence of palladium-catalyzed carbon-nitrogen bond formation, commonly referred to as the Buchwald-Hartwig amination, has revolutionized this field of chemistry. It has become a fundamental synthetic transformation and one of the most extensively employed methods in the pharmaceutical and agrochemical industries.[120]
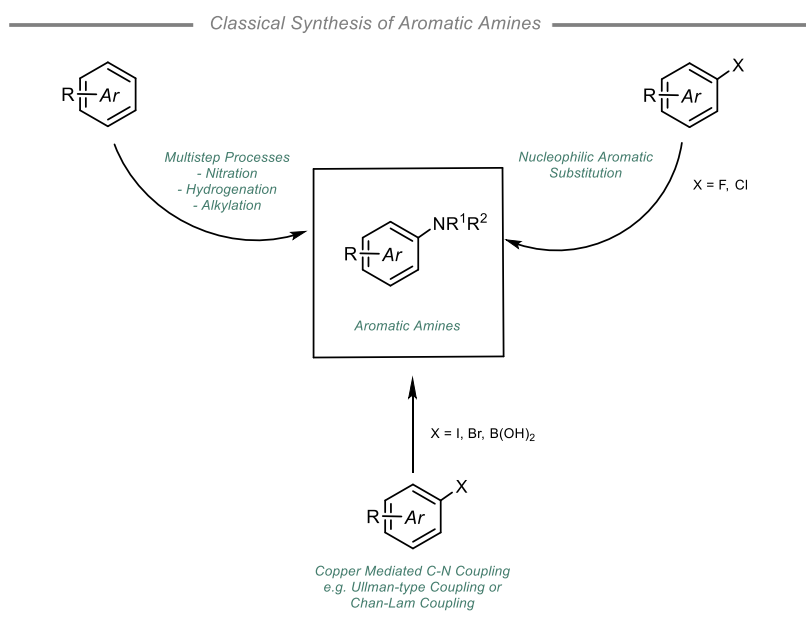


*Scheme 3: Common strategies employed for the synthesis of aromatic amines.*

**a**) Reductive amination
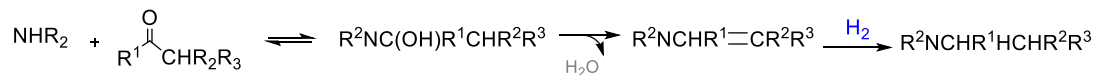


**b**) Buchwald-Hartwig reaction
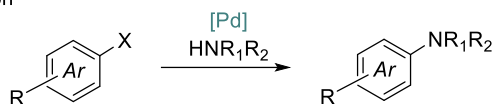


**c**) Petasis synthesis
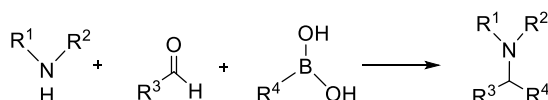


**d**) Eschweiler-Clarke reaction
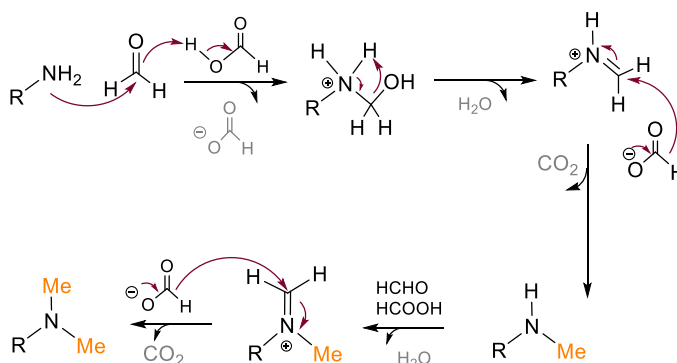


*Scheme 4: Some of the classical synthesis methods of tertiary amines.*

A less familiar method for synthesizing tertiary amines is the Petasis reaction, which offers an alternative approach. This multicomponent procedure, initially documented in 1993, is often termed a "boronic acid Mannich" reaction. It entails the amalgamation of a secondary amine, an aldehyde, and a boronic acid to yield a tertiary amine (Scheme 4c).[121]

The methylation of an amine by methyl iodide, a seemingly straightforward procedure, often yields a mixture of primary, secondary, tertiary amines, and quaternary salt. An alternative method, the Eschweiler-Clarke reaction that is a modification of the Leuckart reaction, offers a more efficient route to tertiary amines (Scheme 4d).[122] By utilizing formic acid and formaldehyde, this approach ensures high yields of tertiary amines while bypassing the formation of quaternary ammonium salts.[123] This method involves the reduction of imine or iminium salt by the formate anion acting as a hydride donor, resulting in a reductive amination process (Scheme 4d). Initially, the reaction between the amine and formaldehyde generates an aminoalcohol intermediate; subsequent dehydration leads to the formation of an iminium ion, then a hydride transfer from the reducing agent to the protonated imine yields the methylated amine. This sequence of reactions iterates until a tertiary amine is produced, halting the process.[123]

## 1.2   Reduction of amides under hydrosilylation conditions

During the second half of the 20th century, progress in transition-metal research, combined with the introduction of silane reagents, played a pivotal role in advancing the carbonyl hydrosilylation reaction, that is the addition reaction of organosilicon compounds containing one or more Si-H bonds to unsaturated organic molecules.[86] In the 1980s and 1990s Cu-,[124] Ir-,[125] Mo-,[126] Rh-,[127] Ru-,[128] Ti-,[129] and Zn-based catalysts were developed for the hydrosilylation of aldehydes, ketones and esters.[130] Over the last decade, significant attention has been directed towards a specific catalytic system employed in amide hydrosilylation, namely Vaska's complex (IrCl(CO)(PPh$_3$)$_2$)[131], in combination with 1,1,3,3-Tetramethyldisiloxane (TMDS).[86]
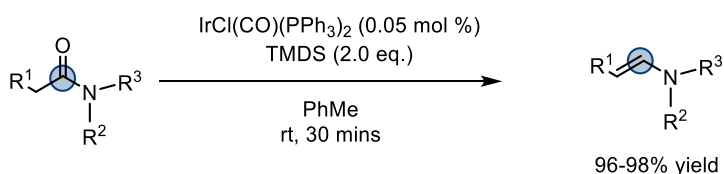


Scheme 5: Vaska's complex catalyzed conversion of tertiary amides to enamines

This system has gained prominence within the synthetic community due to the notable efficiency and chemoselectivity exhibited by Vaska's complex, particularly in tertiary amides, even in the presence of other functional groups. This remarkable performance has resulted in its widespread application in the synthesis of α-functionalized amines, as well as in late-stage chemoselective reductions of amides or lactams.[131] Despite these advancements, amides remained challenging substrates for hydrosilylation until the early 2010s, when Co-, Cu-, Fe-, Mo-, Rh-, Ru-, and Zn-based catalysts were demonstrated to efficiently unlock amides towards hydrosilylation.[132] In fact, the low electrophilic carbonyl of the amide, which is mainly due to its resonance interaction with the lone pair of the vicinal nitrogen, has been a challenging target for hydrosilylation. Thus, clearly amide reduction has undergone thorough examination for the preparation of corresponding amines, imines, or enamines through the cleavage of the C−O bond.[133] Among the diverse methods developed to obtain amines, direct amide reduction to their corresponding amines is one of the fascinating transformation and the most straightforward and efficient approach.[133] However, it presents challenges, often necessitating the utilization of highly reactive stoichiometric reductants like lithium aluminum hydride (LiAlH$_4$)[134] or sodium borohydride (NaBH$_4$),[135] rare transition metal catalysts, or a combination of both, along with harsh reaction conditions.[136] The unveiling of LiAlH$_4$ in 1947 (synthesized by reacting AlCl$_3$ with LiH) [137] and NaBH$_4$ in 1953 (obtained by treating B(OMe)$_3$ with NaH)[138] laid the groundwork for the advancement of novel and highly chemoselective reagents, significantly broadening the range of reducing agents available. Sodium borohydride stands out as the favored reduction reagent on a large scale due to its reliability, wide availability in bulk and diverse forms (including powder, pellets, and caustic solution), and cost-effectiveness, being the most economical metal hydride on an equivalent hydride basis.[135] While the use of LiAlH$_4$ and NaBH$_4$ prove effective, their application is constrained by their vulnerability to air/moisture and their propensity to interact with other functional groups.[135] Diborane, a comparatively gentler reducing agent, has been documented for amide reduction in the presence of esters and nitro groups.[133] In addition, amides pose a challenge in achieving chemoselectivity due to being the least electrophilic among carbonyl species. Moreover, their reactivity hierarchy of tertiary > secondary > primary adds complexity to the reduction process.[136] Hence, the transformations of amides remain a persistent and formidable challenge in the field of organic chemistry.[136] To circumvent stoichiometric conditions, as an alternative to using these reactive reagents, homogeneous and heterogeneous catalytic systems for the

hydrogenation of the amides are developed, employing molecular hydrogen or hydrosilane as hydrogen donors in conjunction with transition metals.[139] Nevertheless, these reactions are conducted under exceedingly high pressures and temperatures, giving rise to safety concerns, challenges in scalability, and limited functional group tolerance.[140] To tackle these issues, researchers have combined transition metals and ligands, along with suitable acid additives, to develop active catalytic systems. Buchwald and colleagues discovered the reduction of tertiary amides to aldehydes with Ph$_2$SiH$_2$ employing a stoichiometric quantity of Ti($^i$PrO)$_4$.[141] A diverse array of amides bearing various functional groups were easily transformed into their respective aldehydes using a straightforward protocol as shown in Scheme 6 below.
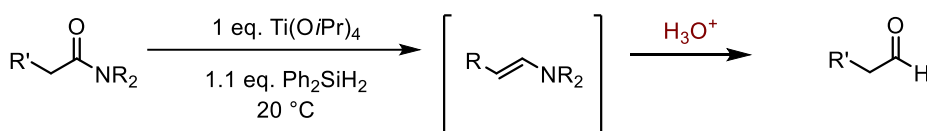


*Scheme 6: Catalytic and stoichiometric titanium-mediated hydrosilylations of amides.*

Usually, the reaction is conducted without a solvent, employing 1.0 equivalent of Ti(O$i$Pr) and 1.1 equivalents of Ph$_3$SiH at room temperature, although THF or benzene can be utilized if preferred. Analysis of the reaction product's $^1$H NMR spectrum with anisole as an internal standard reveals enamine yields within the range of 80-95%, but there are no observed instances of overreduction to amine.[141] Encouraged by this, further efforts were initiated to achieve catalytic reduction using hydrosilanes. Harrod and colleagues reported the Cp$_2$TiF$_2$-catalyzed reduction of tertiary amides to tertiary amines with methylphenylsilane (PhMeSiH$_2$) as illustrated in Scheme 7.[142]
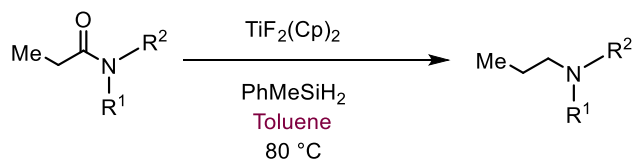


*Scheme 7: Reduction of tertiary amide Cp$_2$TiF$_2$-catalyzed.*

Ito and Ohta et al. demonstrated that rhodium-triphenylphosphine complexes also serve as effective catalysts for reducing tertiary- and secondary amides using diphenylsilane ($Ph_2SiH_2$) as a reducing agent (Scheme 8).[143]
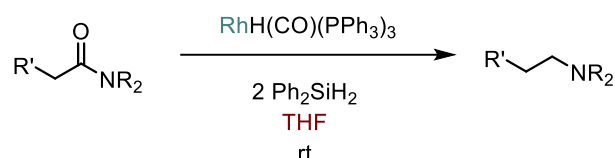


*Scheme 8: Reduction of tertiary-secondary amide RhH(CO)(PPh3)3 -catalyzed.*

In 2001 Fuchikami et al. reported that several metal complexes of groups 7-10 (mostly Mn, Os and Rh) catalyzed the reduction of amides with tryethylsilane ($Et_3SiH$).[144] The authors elucidated a development: the Rh-complex-catalyzed reduction of tertiary amides to amines, employing $H_2SiPh_2$ or $H_3SiPh$ as reagents. Notably, only one of the H-Si bonds participates in the reaction, and room temperature reactions are unattainable with monohydrosilane, despite its greater stability and lower cost compared to polyhydrosilanes.[143] They utilised monohydrosilanes as reducing agents at elevated temperatures, and, regrettably, the necessity for such elevated temperatures in the reaction is somewhat its Achilles' heel.[144] The general reaction is summarized in Scheme 9 below.
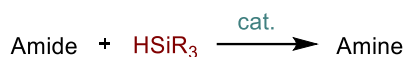


*Scheme 9: General reaction of hydrosilylation of amides with hydrosilanes.*

In 2007 the reduction of tertiary and secondary amides with phenylsilane ($PhSiH_3$) was accomplished by catalysis of $MoO_2Cl_2$.[145] In 2009, H. Nagashima et al. showed that a triruthenium cluster, $(\mu3,\eta2:\eta3:\eta5\text{-acenaphthylene})Ru_3(CO)_7$, efficiently catalyzes the reduction of carboxylic acids, esters, and tertiary amides with hydrosilanes (Scheme 10).[69]
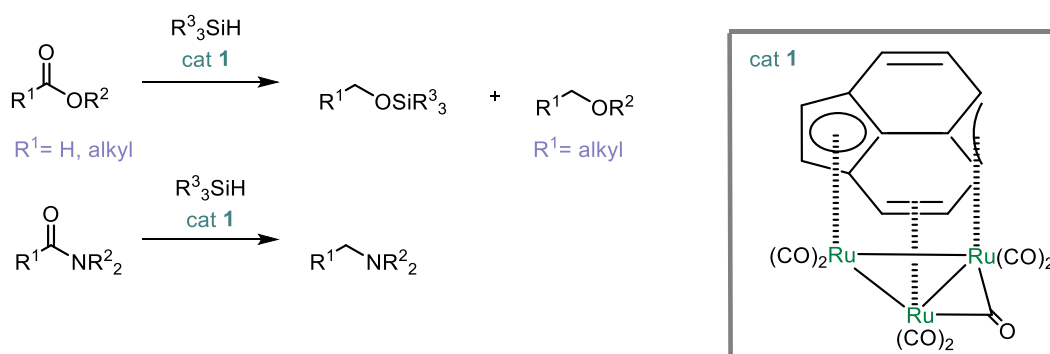
*Scheme 10: Reduction of amide and esters with hydrosilanes and Ru-based catalyst.*

In 2013, Cole-Hamilton and colleagues reported the deoxygenative hydrogenation of amides catalyzed by [Ru(acac)$_3$] and triphos with methanesulfonic acid, as shown in Scheme 11.[85]
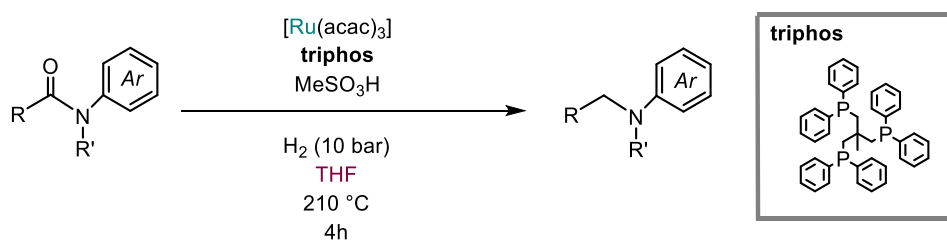


*Scheme 11: Deoxygenative hydrogenation of amides with Ru-based catalyst.*

Since this breakthrough, numerous research groups have devised metal-mediated hydrosilylation employing various metals like Rh,[143] Ru,[146] Zn,[147] Pt,[69] Mn,[148] Ir,[149] Zr,[150] and Ni.[151] It is widely acknowledged that certain transition metal salts and complexes serve as effective catalysts for hydrosilylation.[57] Additionally, metal-free procedures have also arisen to modulate reactivity, employing organocatalysts like B(C$_6$F$_5$)$_3$,[152] Tf$_2$O,[153] Et$_3$B,[154] NaEt$_3$BH,[155] BPh$_3$,[156] and TBAF.[157] Charette and co-workers developed metal-free reduction of tertiary and secondary amides using a stoichiometric amount of triflic anhydride (Tf$_2$O) with hydrosilanes and the Hanzsch ester as hydride donors (Scheme 12).[136]
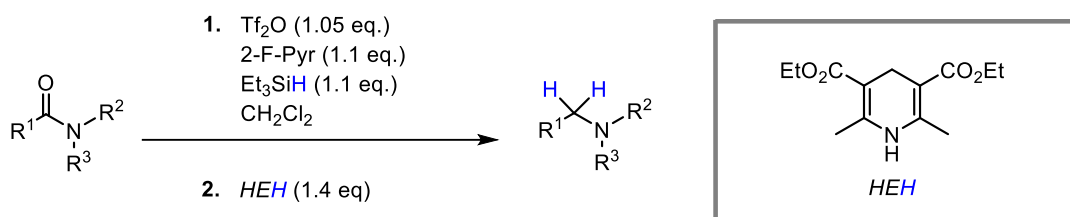
*Scheme 12: metal-free reduction of tertiary amides.*

Numerous efforts to develop catalytic metal-free conditions have been reported so far, like various approaches, including the utilization of Brønsted or Lewis acids for system activation, alongside the potential catalytic role of inorganic bases, have been explored. The achievement of chemo- and site-selective reductions is realized through the synergistic interplay of silanes, catalysts, and specific reaction conditions, catering to tertiary, secondary, and, in exceptional instances, primary amides. The use of bases like KO$^t$Bu, KOH, and Cs$_2$CO$_3$ are also reported for hydrosilylation reactions. In 2013, Beller and colleagues discovered that a benzothiophene-derived boronic acid efficiently catalyzed the hydrosilylation of amides.[158]
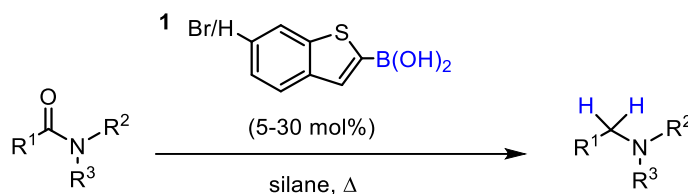


*Scheme 13: reduction of amides with benzothiophene-derived boronic acid.*

This reaction proved successful for various tertiary amides and exhibited tolerance to a broad spectrum of functional groups, including secondary and primary amides. This method is operationally simple, safe, gives less byproducts, although a higher catalyst amount was required (*20 mol%* for secondary and *30 mol%* for primary amides) as is shown in Table 1 below.[158]

*Table 1: Hydrosilylation of tertiary, secondary and primary amides.*

| Amide | Conditions | Examples | Results |
|---|---|---|---|
| Tertiary | **1** (*5-10 mol%*), PhSiH$_3$ (2.4 equiv.) Toluene, 110–130 °C, 36 h.[158] | 10 | Up to 98% yield |
| Secondary | **1** (*20 mol%*), PhSiH$_3$ (2.4 equiv.) Toluene, 130 °C, 24–40 h.[158] | 6 | Up to 89% yield |
| Primary | **1** (*30 mol%*), PhSiH$_3$ (3 equiv.) Toluene, 110–130 °C, 24 h.[158] | 4 | Up to 63% yield |

Recently, Chung Whan Lee and Haye Min Ko have developed a dual photoredox/nickel-catalytic system for the chemoselective reduction of amides.[159] Nagashima and co-workers used commercially available and inexpensive TMDS, that is a practically useful reductant, and several Pt compounds as catalysts such as H$_2$PtCl$_6$·6H$_2$O, Karstedt's cat., Pt(dba)$_2$, PtCl$_2$(cod) and Pt/C.[69]
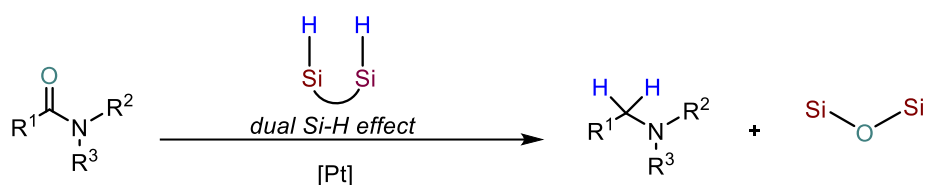


*Scheme 14: general reaction of the Pt-based catalyzed Reduction of Tertiary Amides with the "dual Si-H effect".*

Stable hydrosilanes are advantageous for handling, and the reduction reported by them is tolerant to several reducible functional groups such as $NO_2$, CN, esters, and halides.[69] Reaction proceeds under mild conditions, showing high amido-group selectivity in the presence of other reducible functional groups. With all the platinum catalysts, including heterogeneous Pt/C, conversion of the amide reached over 89% after 5 h, but there is a side reaction that produce a small amount of the enamine.[69] The same group tried in a previous work a Ruthenium cluster-catalyzed reduction of amides, but reduction of secondary amides did not take place under the same conditions as those with tertiary amides. Consequently, they have solved this issue by combining the "dual Si-H effect" and a higher concentration of the catalyst (3 mol%) at a slightly elevated temperature. The topic of the dual Si-H effect will be further explored in more depth in the dedicated chapter "The use of silanes and the dual Si-H effect".
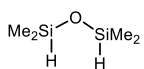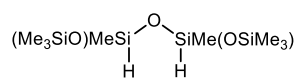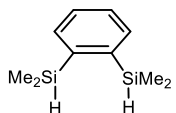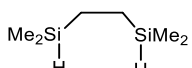
## 1.3  The use of silanes and the dual Si-H effect

Recently, addressing the removal of metal catalysts and residual reactants from products has gained recognition as an environmental concern. While conventional hydride reduction using $LiAlH_4$ proves useful for laboratory-scale experiments, its sensitivity to oxygen and moisture, along with challenges in separating aluminum wastes from the product, present drawbacks. A promising alternative involves the catalytic hydrosilylation of amides using commercially available hydrosilanes as reductants.[139] Although silanes are generally unreactive and necessitate activators to function as a reductant in the catalytic cycle, the integration of precious metal catalysts alongside diverse ligands, has been proven effective for the efficient reduction of amides.[136,139] The reduction of carbonyl compounds with silanes in acidic conditions has been acknowledged since the 1970s. Given the superior handling convenience of hydrosilanes compared to traditional hydride reagents, the current platinum-catalyzed reduction of amides with hydrosilanes deserves further attention, particularly when the reaction can be adapted for the large-scale production of amines.[69] A pivotal discovery in the reduction of amides to amines under mild conditions with a Pt-based catalyst was the "dual Si-H effect," where two adjacent Si-H groups collaboratively accelerate the reaction.[160] A significant acceleration in reaction rate is noted when utilizing hydrosilanes containing these dual Si-H groups, facilitating the reduction of secondary amides to secondary amines (a result not achievable with

standard monohydrosilanes under mild conditions).[69] Use of hydrosilanes containing two proximate Si-H groups in a molecule such as TMDS and 1,2-bis(dimethylsilyl)benzene made the reduction of amides possible in the presence of commercially available platinum compounds such as Speier's and Karstedt's catalyst.[69] Notably, the practical advantage lies in the use of cost-effective TMDS as the reductant, with the added benefit of automatic removal of silicone and platinum species from the product when PMHS, that is the TMDS polymeric equivalent, is employed.[161]

The observation of the "dual Si−H effect" in the platinum-catalyzed reduction of amides was investigated by Nagashima et al. reacting *N*,*N*-dimethyl-3-phenylpropionamide (**1a**) with various hydrosilanes (Si−H = 3 equivalent to **1a**) using $H_2PtCl_6 \cdot 6H_2O$ (1 mol%) as a catalyst in THF at 50 °C (Table 2). No reaction occurred when hydrosilanes containing only one Si−H group in the molecule were employed, such as $PhMe_2SiH$, $EtMe_2SiH$, $(EtO)_3SiH$, or $Me_3SiOSiMe_2H$, as illustrated in entries 1 to 4. Despite $Ph_2SiH_2$ being recognized as a potent reducing agent in numerous transition metal-catalyzed reductions of carbonyl compounds, only the initial amide was recovered completely under these conditions (entry 5). In sharp contrast, reactions utilizing hydrosilanes containing two proximal Si−H groups in the molecule resulted in the formation of *N*,*N*-dimethyl-3-phenylpropylamine (**2a**) in satisfactory to excellent yields.[69] The reactivity versus structure of the hydrosilane exhibits notable distinctions from the findings previously reported in the $RhCl(PPh_3)_3$-catalyzed hydrosilylation of ketones[162] and the $[Ru_3]$ cluster-catalyzed hydrosilylation of carbonyl compounds.[163] In these prior instances, $Me_2HSi(CH_2)_2SiHMe_2$, which generally displayed reactivity as a hydrosilane, did not demonstrate effectiveness in the platinum-catalyzed reduction of amides (entry 9). This observation suggests that the sensitivity of " the dual Si−H effect " in platinum-catalyzed reduction may be more pronounced in relation to the distance between two Si−H groups compared to reactions catalyzed by [Rh] or $[Ru_3]$.[69]

*Table 2: Structural effect of hydrosilanes.*

| Entry | Hydrosilane | Yield (%)[a] |
|:---:|:---:|:---:|
| 1 | PhMe$_2$SiH | <1 |
| 2 | EtMe$_2$SiH | <1 |
| 3 | (EtO)$_3$SiH | <1 |
| 4 | Me$_3$SiOHMe$_2$H | <1 |
| 5 | Ph$_2$SiH$_2$ | <1 |
| 6 | Me$_2$Si—O—SiMe$_2$ (H, H) | > 98 |
| 7 | (Me$_3$SiO)MeSi—O—SiMe(OSiMe$_3$) (H, H) | >98 |
| 8 | Me$_2$Si—SiMe$_2$ (benzene ring, H, H) | >98 |
| 9 | Me$_2$Si—CH$_2$CH$_2$—SiMe$_2$ (H, H) | <1 |

[a] Determined by $^1$H NMR analysis with ferrocene as an internal standard.

# Chapter 2

*Experimental part*

## 1.1  This work

In this project of thesis platinum-based catalysts were used for the reduction of amides, in particular the *N,N*-dimethylacetamide was used as substrate in order to optimize the reaction and subsequently apply the reaction to additional substrates. The catalysts are the same employed in the hydrosilylation reaction and they are described in the preceding chapter.

## 1.2  The optimization of the reaction

Typically, the optimization of chemical reactions relies on empirical methods, where chemists experiment with operational parameters based on their understanding of the reaction, aiming to achieve optimal outcomes.[164] A persistent challenge in applied physical and chemical sciences pertains to the identification and synthesis of chemical compounds or materials possessing optimal properties for specific applications. A considerable portion of research in physics, chemistry, and materials science revolves around the exploration and characterization of novel compounds that could serve societal needs, yet much of the progress still relies on trial-and-error experimentation, incurring substantial time and financial costs. This conventional approach can be demanding in terms of time and resources, as small adjustments to various factors can have a significant impact on production.[165] Machine Learning (ML) models stand poised to revolutionize the landscape of chemical sciences by significantly expediting computational algorithms and augmenting insights derived from computational chemistry techniques.[166] Nonetheless, realizing this potential necessitates a collaborative synergy between expertise in computer science and physical sciences. Given the pressing global challenges, there is an escalating urgency for research and development endeavors that are faster, more efficient, and economically viable. Over time, computational chemistry (*CompChem*) methods have

witnessed significant advancements, holding the promise of paradigmatic shifts in the fundamental understanding and tailored design of compounds for targeted applications.[165] ML offers a solution by establishing intricate patterns among different process variables, swiftly identifying the optimal operating point, and guiding a smart and efficient experimental campaign.[167]

In this thesis project, ML was employed to optimize the conditions of the reduction reaction from amides to amines, with the aim of saving time, materials, costs, and placing greater emphasis on avoiding waste and the use of non-green substances or methods. The substrates that were utilized are the *N*,*N*-dimethylacetamide and the TMDS (Scheme 15), and the reaction was conducted with five different Pt-based catalysts.
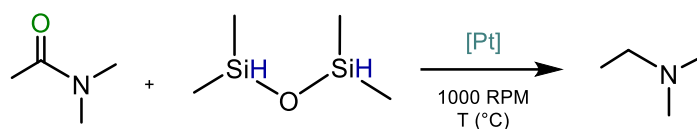


*Scheme 15: reduction of N,N-dimethylacetamide with TDMS.*

To optimize the reaction, we collaborated with the Sunthetics Inc team that uses this platform for developing and exploiting algorithms capable of optimizing chemical reactions in the shortest possible time. It combines traditional Artificial Intelligence (AI) with physical insights to develop new chemical products, processes, and reactions. This will be further explored in one of the subsequent chapters.

# 1.3  What is Machine Learning?

A Machine Learning Algorithm is an algorithm that can learn from data. But what do we mean by *learning*? It can be explained with the succinctly articulated by Mitchell (1997): "*A computer program is said to learn from experience E with respect to some class of tasks T and performance measure P, if its performance at tasks in T, as measured by P, improves with experience E*".[166] This definition encapsulates the essence of machine learning, where algorithms are designed to enhance their performance over time through exposure to data and experience. The improvement in performance is typically gauged by a predefined measure, P, which reflects the algorithm's ability to excel at the tasks within the specified class T. Since the inception of computers, there has been a longstanding curiosity about their potential for learning. The prospect of programming them to autonomously improve with experience has been a subject of considerable interest. Envision a scenario where computers learn from medical records to discern the most effective treatments for emerging diseases, or houses learning from experience to optimize energy costs by adapting to the specific usage patterns of their occupants. The transformative impact of such learning capabilities is profound.[168] ML is something like that, it is a system that learns during the process. ML finds applications across various technological fields, including but not limited to web search, translation, natural language processing, self-driving vehicles, and control architectures. ML finds applications across various technological fields, including but not limited to web search, translation, natural language processing, self-driving vehicles, and control architectures. In the sciences field, ML is extensively employed in medical diagnostics, reconstructing brain circuits, and predicting the effects of mutations in non-coding DNA on gene expression and disease,[169] particle physics,[170] nano sciences,[171] bioinformatics,[172] brain-computer interfaces,[173] social media analysis, robotics,[174] and team, social, or board games.[175,176] Notably, these methods have gained popularity for their effectiveness in expediting the discovery and design processes associated with new materials, chemicals, and chemical processes.[177] ML has undeniably exerted a profound impact on various facets of our daily lives, emerging as one of the most pervasive technologies in our era. Its significance is difficult to exaggerate, particularly in addressing persistent challenges within computer science. Notably, ML has played a pivotal role in tackling issues such as image classification and natural language processing, tasks that demand a level of understanding that traditional computer programs find challenging to capture. In contrast to previous classical artificial intelligence (AI) approaches, which heavily relied on extensive

sets of rules and heuristics, ML has proven to be more adept at handling the intricate nuances of complex problems that were previously beyond the reach of conventional methods.[169] In recent decades, advancements in ML algorithms and computer technology have facilitated the extraction of underlying regularities and meaningful patterns from extensive datasets. This capability enables the automatic construction of potent models, often surpassing human performance in certain tasks.[177] This progress has inspired researchers to apply the same tools to address scientific challenges, fueled by the optimism that ML could revolutionize their respective fields in a comparable manner. For all intents and purposes, ML algorithms operate by estimating functional relationships in data without explicit instructions on how to analyze or draw conclusions. Learning algorithms have the capacity to deduce mappings between sets of inputs and corresponding outputs or even from inputs alone. In the absence of output labels, the algorithm autonomously discovers structure within the data. Regression analyses focus on reconstructing the function that passes through a set of known data points with the least error. In contrast, ML techniques aim to identify functions that can predict interpolations between data points, thereby minimizing prediction errors for new data points that may emerge later. The emphasis is on creating models that generalize well to handle unseen data, extending beyond the specific points used in training.[177]

## 1.4   Disadvantages and limitations

Certain challenging problems in chemistry and physics could be accurately addressed using *Comp-Chem* but doing so would demand substantial resources. An example is the unavoidable quadratic scaling in enumerating all pairwise interactions in a many-body system. Unfortunately, there is no apparent workaround for this challenge.[168] One might consider whether empirical approaches could offer more efficient solutions to such fundamental problems. However, this is not feasible because ML is better suited for finding solutions in general function spaces rather than in deterministic algorithms where constraints guide the solution process. Nevertheless, if the goal is not to find a complete solution but rather some aspect of it, the stochastic nature of ML can be advantageous. For instance, a traditional ML approach might not be the optimal tool for explicitly calculating the *Schrödinger equation*, but it can be a far more useful tool for developing a force field that provides the

energy of a system without the need for a cumbersome wavefunction and a self-consistent algorithm.[178] ML algorithms demand a substantial quantity of high-quality data, and determining in advance when a dataset is adequate can be hard. Indeed, there are situations where a dataset may be extensive in size, but it may not sufficiently sample all the relevant systems one intends to model.[177]

## 1.5   What Does ML Do Well?

ML excels at extracting implicit knowledge from data by inferring functional relationships in a statistically rigorous manner, even in the absence of detailed knowledge about the specific problem at hand. It has the capability to capture implicit knowledge from a dataset, including aspects where prior domain-specific knowledge might be lacking. In contrast to traditional modeling approaches, ML algorithms exhibit versatility in their approach, starting from a generalized model and loss function. With increasingly larger and informative training datasets, generalization can be improved to arbitrary accuracy within the bounds of inherent data noise. This iterative process enables the exploration of a problem even before a comprehensive understanding is achieved. An ML predictor can serve as a foundational element in the modeling loop, facilitating the construction of predictive models, their improvement, enrichment through formal insights, and continuous refinement to ultimately extract a formal understanding. As research efforts evolve, there is a growing trend to combine data-driven learning algorithms with rigorous scientific or engineering theory, leading to the generation of novel insights and applications. This interdisciplinary approach enhances the synergy between data-driven methods and established theoretical frameworks, contributing to a deeper understanding of complex systems.[177]

## 1.6 The need for behavioral change and adoption of novel tools

The production of chemicals is essential for the manufacture of everyday items, spanning electronics, textiles, and food.[165] The chemical industry has emerged as the third-largest contributor to greenhouse gas emissions, with over half of its resources ending up as waste.[57] It is clear how much it is important and urgent to find a way to speed up the optimization of chemical processes, avoiding several test-error-rejection steps. In applied physical and chemical sciences an obvious question comes to mind: how to identify and create chemical compounds or materials with optimal properties for specific purposes? A considerable portion of research in physics, chemistry, and materials science revolves around discovering and characterizing novel compounds that can benefit society. However, the predominant approach still relies on trial-and-error experimentation, demanding significant time and resources. In the face of current global challenges, there is a growing need for research and development efforts that are faster, more effective, and cost-efficient.[177] *CompChem* methods have undergone substantial improvement over time, holding the promise of bringing about paradigm shifts in the fundamental understanding and design of compounds tailored for specific applications. Concurrently, ML methods have experienced an unprecedented technological evolution in recent decades, leading to a multitude of applications that have seamlessly integrated into our daily lives.[169]

## 1.7 What is Sunthetics?

In this thesis project there was a collaboration between *UGent* University and the easy-to-use machine learning platform: Sunthetics.[179] Accelerating innovation to enhance materials and streamline processes is the most efficient strategy for achieving enduring sustainability. [168] Historically, this innovation journey has been prolonged, often spanning years due to the extensive experimentation needed to create a viable and marketable product. Additionally, conventional predictive modeling tools, whether physical, statistical, or machine-learning based, require a deep comprehension of reactions or a vast array of data points to yield valuable insights.[179]

# 1.8 The acceleration in the chemistry industry by Sunthetics

Sunthetics has substantially diminished the number of trials required for chemical process optimization by up to fivefold. This advanced ML platform is designed to aid in the development of new materials, processes, and formulations, utilizing a minimal dataset for accurate predictions of system behavior. At the convergence of chemical engineering and Bayesian Optimization, it harnesses a synergy of principles from both domains, deploying advanced predictive ML algorithms. Achieving up to 15 times faster R&D, the software not only enhances existing manufacturing processes but also unlocks unprecedented performance and, additionally, it proves valuable in identifying anomalies and facilitating diagnostics.[179] Chemical reaction optimization often relies on empirical methods, involving manual experimentation with operational parameters. This proves time and resource-intensive due to the significant impact of small adjustments on production outcomes.[164] ML offers a solution by identifying intricate patterns among process variables, swiftly pinpointing the optimal operational point, and guiding an intelligent experimental campaign.[166] It requires no ML knowledge, making it user-friendly for chemists and engineers. By prioritizing cost and efficiency, these tools reduce expenses, improve efficiency, and lower carbon emissions, energy, and raw material usage.[179] The Sunthetics platform, accessible via a web browser, is reaction agnostic, enabling impact across various chemical industry sectors quickly.[179] There are generally two approaches to providing interpretable ML: the model-agnostic and model-specific approaches.[180] The model-agnostic approach is not tied to the specifics of a particular ML model, it's designed to be broadly applicable across various types of models; it can be applied to any black-box ML system represented as f(x), where the term "black-box" refers to a model where the internal workings are not transparent or easily understandable. The goal of model-agnostic methods is to provide interpretability without relying on the inherent structure or details of a specific ML model. These methods are more generic and can be used across different domains and models.[181] This type of approach exhibits versatility by being applicable across a broad spectrum of chemical reactions without predisposition to a particular subset, like in Sunthetics platform.[180] A reaction-agnostic platform in chemistry may, for instance, manifest as a sophisticated tool or software leveraging machine learning methodologies for the optimization of diverse chemical reactions. By contrast, the model-specific approach involves methods that are tailored to a particular ML model used within a specific domain. This approach utilizes a domain-specific

ML system, meaning the methods are designed with the details and structure of a particular model in mind. The model has characteristics that are meaningful within the specific domain of interest. The aim of model-specific approaches is to leverage the knowledge about the structure of the ML model to provide interpretable insights.[181] Sunthetics ML accelerates innovation by transforming the way you operate in the lab. It is a tool to access predictive power of AI using smaller data set. When the algorithm is then applied, it creates a complete set of performance predictions, and provides recommendations for subsequent experiments to run that will lead to reduced uncertainty in the system and improve prediction accuracy with as few experiments as possible.

# 1.9  The application of Sunthetics in the project

The platform works in this way: the number and the type of variables that the algorithm can control has to be chosen. We set three variables: time, in a range from 1 to 24 hours, temperature, in an interval from room temperature (25 °C) to 80 °C and catalyst loading from a minimum of 0.05 mol% to a maximum of 1.00 mol%. After each reaction, based on the conversion, TOF and TON, the algorithm suggests what it "thinks" are the best conditions, changing the values of the three chosen variables, thus suggesting reactions with different temperatures, time, and catalyst loading. In Table 1, the first ten reactions that the algorithm suggested are reported. The first one is the only one that was conducted with PHMS instead of TDMS, because it is a cheap silane as it is a waste product from the silicone industry. Unfortunately, it did not work because it tends to cross-link and solidify in the presence of a platinum-based catalyst, in fact conversion to the desired product was not observed (see entry 1).

*Table 1: first ten reactions suggested by the algorithm.*

| Entry | Catalyst | Cat. Loading (mol%) | Time (h) | T(°C) | Conversion (%) | TON | TOF (h$^{-1}$) |
|-------|----------|---------------------|----------|-------|----------------|-----|-----------------|
| 1 | [Pt(DMS)$_2$Cl$_2$]* | 1.00 | 21 | RT | NR | / | / |
| 2 | [Pt(DMS)$_2$Cl$_2$] | 0.70 | 7 | 30 | **>99** | 141 | 20 |
| 3 | [Pt(ICy)(DMS)Cl$_2$] | 1.00 | 2 | 50 | 48 | 48 | 24 |
| 4 | [Pt(IMes)(DMS)Cl$_2$] | 0.50 | 22 | 70 | 60 | 120 | 5 |
| 5 | [Pt(SIPr)(DMS)Cl$_2$] | 0.80 | 18 | 50 | 36 | 45 | 2 |
| 6 | [Pt(DMS)$_2$Cl$_2$] | 0.15 | 3 | 34 | **>99** | 667 | 222 |
| 7 | [Pt(ICy)(DMS)Cl$_2$] | 0.35 | 2 | 60 | NR | / | / |
| 8 | [Pt(IMes)(DMS)Cl$_2$] | 0.55 | 23 | 66 | 52 | 94 | 4 |
| 9 | [Pt(SIPr)(DMS)Cl$_2$] | 0.95 | 7 | 40 | 30 | 31 | 4 |
| 10 | [Pt(THT)$_2$Cl$_2$] | 0.50 | 20 | 50 | **>99** | 200 | 10 |

*\*For this reaction PHMS as silane was used instead of TMDS.*

# 2  Conversion

In the realm of organic chemistry, the determination of percent conversion via Nuclear Magnetic Resonance (NMR) spectroscopy often involves comparing the integrated areas beneath the respective peaks corresponding to the reactant and product. Despite NMR's inherent limitations in quantitative analysis, this method enables an estimation of the extent of reactant transformation into product. The first thing to do is to select distinctive and representative peaks for both the starting material and product. Upon conducting the reaction and acquiring the sample, NMR analysis is performed, wherein the targeted peaks are integrated. It is essential to standardize the integration of multiproton entities to unity (i.e., if there is a methyl group is needed to divide the integral of the methyl group by 3). The ratio of normalized peaks pertaining to the starting material and product reflects the ratio of these entities. Subsequently, the percent conversion is determined by the ratio of product peak area to the combined areas of starting material and product. This methodology serves as a prevalent means in organic chemistry for monitoring the advancement of chemical transformations. In this work the conversion was always calculated by $^1$H NMR (80 MHz). Specifically, it involves monitoring the emergence of characteristic peaks corresponding to the product (the amine) and the disappearance of peaks indicative of the substrate (the amide). The Figures 1 and 2 below display two $^1$H NMR spectra: the first spectrum corresponds to the *N*,*N*-dimethylacetamide, the substrate employed, as evidenced by the characteristic peaks at 2.14 and 3.03 ppm. The second spectrum represents an instance of a reaction with complete conversion, wherein the distinctive amine peaks at 2.23, 1.00 and 2.42 ppm are observable, alongside the TMDS peaks, and the substrate peaks are no longer evident (Figure 1 and 2).
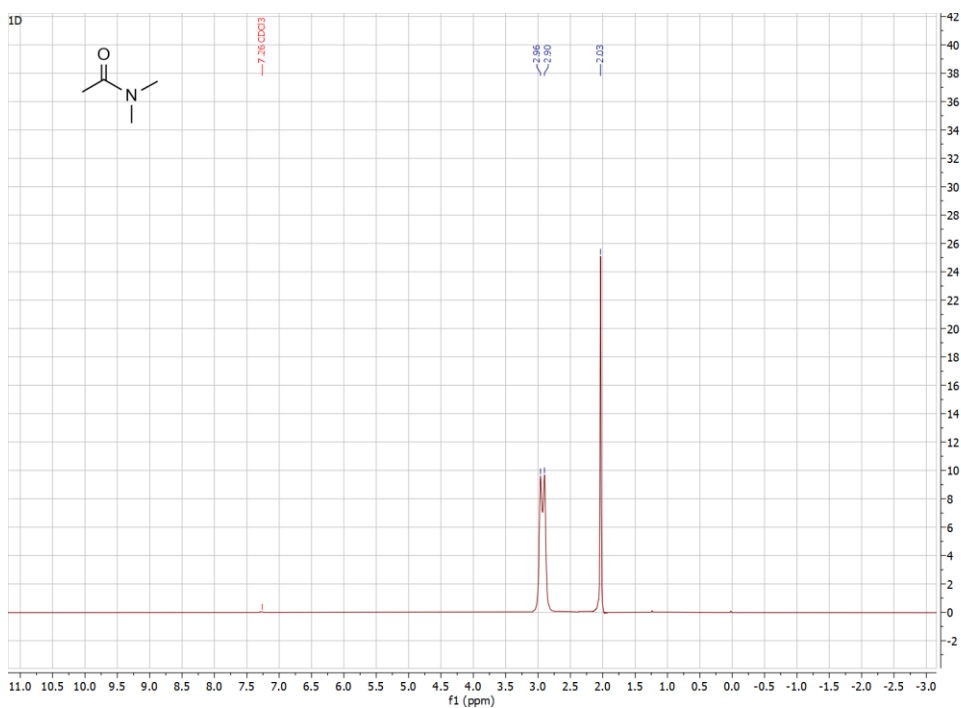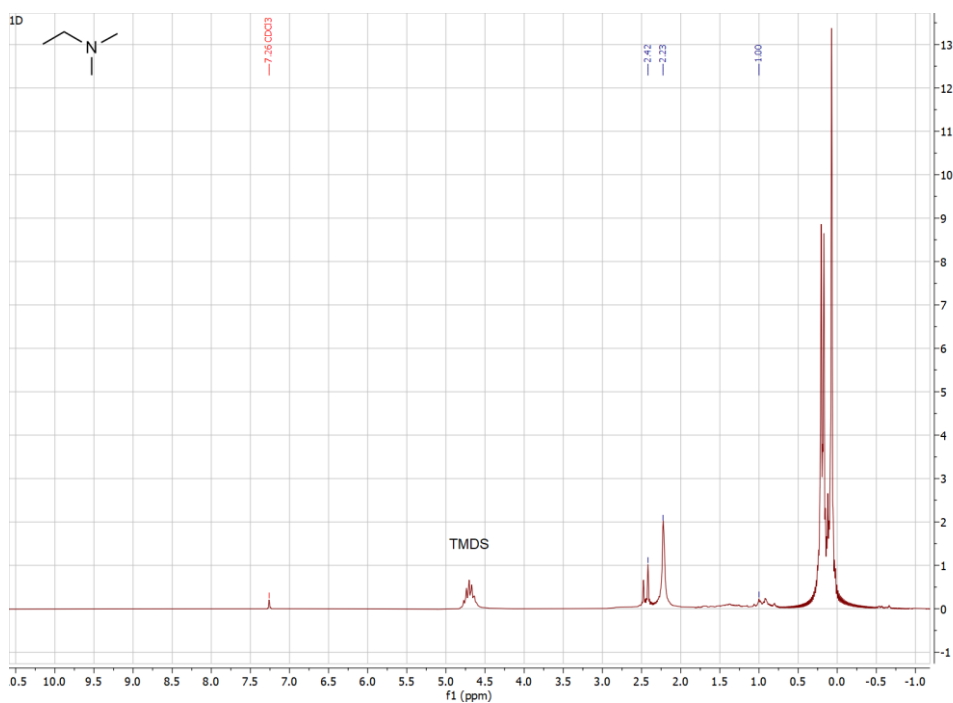
*Figure 1: spectrum of the substrate.*



*Figure 2: spectrum of the final amine.*

68

## 2.1 Turnover Frequency and Turnover Number

*"Indeed, the catalytic activity, for a valid comparison, must be referred to the number of exposed surface atoms of a specified kind. Thus, a convenient way to express catalytic activity is by means of a turnover number equal to the number of reactant molecules converted per minute per catalytic site for given reaction conditions."* [182]

These Boudart's words marked the initial establishment of what would later be termed Turnover Frequency (TOF) within the field of heterogeneous chemistry. Originating from enzymatic kinetics, this term gradually transitioned into the domain of catalysis.[183] Although widely utilized, the concept of "turnover frequency" remains ambiguously defined. One initial issue with this interpretation is that as indicated in Boudart's words, the terms "turnover frequency" (TOF) and "turnover number" (TON) may initially appear to be synonymous.[184] The misinterpretation of these terms is understandable considering that one finds ambiguous definitions in reliable sources of information. As an example, the IUPAC Gold Book defines the TOF as "Commonly called the turnover number, N, and defined, as in enzyme catalysis, as molecules reacting per active site in unit time".[185] Judging from this description, it seems that the TOF and the TON are the same, but in the context of catalysis they are not, infact these expressions carry distinct connotations. In biochemistry the term TON is still, regretfully, used with the same meaning as TOF.[186] Although this old definition of TON predates the current use by the homogeneous and heterogeneous community, the confusion should be avoided by taking into account the name of the quantity: the TOF is a frequency, with units of [time$^{-1}$], while the TON is a dimensionless number.[187] Therefore, the TOF is the measure of the instantaneous efficiency of the catalyst, the TON deals with its lifetime robustness. It corresponds to the total number of turnovers the catalyst can achieve until its total decay, regardless of time.[184] In enzymatic catalysis it is commonly known as total turnover number (TTN),[188] to distinguish it from the TON in the biochemical sense. The TON specifies the maximum use that can be made of a catalyst for a special reaction under defined reaction conditions by the number of molecular reactions or reaction cycles occurring at the reactive center up to the decay of activity. In this respect, the TON represents the maximum yield of products attainable from a catalytic center. The TON results from multiplication

of the TOF [time$^{-1}$] and the lifetime of the catalyst [time].[184] In this project the calculation of TON and TOF was done by the algorithm using the following equations:

$$TON = \frac{Conversion}{Cat\ loading}$$

$$TOF = \frac{TON}{time}$$

## 2.2  Preliminary analysis finding

After the initial eleven responses, the algorithm yielded its incipient outcomes. The correlation graph depicting the relationships between various variables and the target is presented in Figure 3, revealing a correlation coefficient of 0.94 between TOF and TON. Given the correlation between these two factors is so high, one of them can be removed from the optimization.
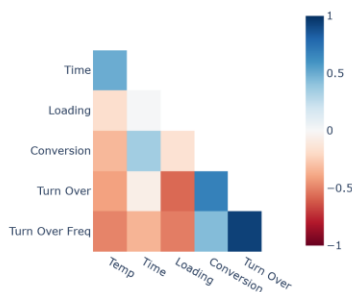


*Figure 3: correlation graph.*

Following this, the model error is presented detailing RMSE and R-squared values for each target, namely Conversion, TON, and TOF.

Table 2: model error with the average R-squared and RMSE for every target

| | Conversion | TOF | TON |
|---|---|---|---|
| *R-squared* | 0.27 ± 0.39 | 0.60 ± 0.55 | 0.39 ± 0.56 |
| *RMSE* | 0.32 ± 0.09 | 27.01 ± 30.39 | 125.87 ± 75.52 |

*Root Mean Square Error* (RMSE) is a commonly used metric to measure the accuracy of a predictive model, particularly in the context of regression analysis. It quantifies the difference between the predicted values and the actual values of a variable. The formula for RMSE is as follows:

$$RMSE = \sqrt{\sum_{i=1}^{n} \frac{(\hat{y}i - yi)^2}{n}}$$

where N is the number of data points, y(*i*) is the *i*-th measurement, and $\hat{y}$(*i*) is its corresponding prediction. Lower RMSE values indicate better agreement between predicted and observed values, with a value of 0 indicating a perfect fit. However, it is important to note that RMSE is sensitive to outliers, as the squared term magnifies large errors. In practice, RMSE is a widely used measure for assessing the performance of regression models. *R-squared* (coefficient of determination) is another metric used in regression analysis to evaluate the goodness of fit of a model. [189] The formula for *R-squared* is as follows:

$$R^2 = 1 - \frac{SSres}{SStot} = 1 - \frac{\sum_i (yi - \hat{y}i)^2}{\sum_i (yi - \bar{y}i)^2}$$

Where *SSR* (Sum of Squared Residuals) is the sum of the squared differences between the observed (actual) values and the predicted values and *SST* (Total Sum of Squares) is the sum of the squared differences between the observed values and the mean of the observed values. The *R-squared*

measures the proportion of the variance in the dependent variable that is explained by the independent variables in the model. *R-squared* values range from 0 to 1, where:

- $R^2$=0: The model does not explain any of the variability in the dependent variable.
- $R^2$=1: The model explains all the variability in the dependent variable.

The algorithm employed utilizes the *Bootstrapping* method for its estimation. *Bootstrapping* is a resampling technique used in statistics to estimate the variability or uncertainty of a statistic or model parameter by repeatedly drawing random samples (with replacement) from a given dataset. This involves creating multiple resampled datasets, analyzing each one, and then using the distribution of results to assess the stability and reliability of the statistic, such as *R-squared* or *RMSE*.[179] This technique improves the robustness and reliability of models by creating multiple datasets through random sampling with replacement and is particularly beneficial for assessing the stability of model performance and estimating the uncertainty associated with model predictions.[190] When *bootstrapping* is employed to estimate error metrics, the variance reflects the stability and uncertainty associated with the model. The term "variance" here does not refer to statistical variance but rather to the spread or inconsistency in the model's predictions, so a lower variance is generally desirable, indicating more consistent and reliable model performance.[190] In this case there is a lot of variance in the error metrics and this is probably because of the time series component. That is why in the next set of suggested reactions each unique experiment has the same time intervals, in fact an $^1$H NMR spectrum was taken after 2 hours per experiment.

## 2.2  Results

The next set of reaction suggested by the algorithm are reported in Table 3. Following the execution of these initial five reactions, the outcomes were conveyed to *Sunthetics* for analysis. Subsequently, based on their assessment, an additional set of five reactions was recommended, and the corresponding results are presented in Table 4.

*Table 3: next five reactions suggested by the algorithm.*

| Entry | Catalyst | Cat. Loading (mol%) | Time (h) | T (°C) | Conversion (%) | TOF |
|-------|----------|---------------------|----------|--------|----------------|-----|
| 1 | [Pt(DMS)$_2$Cl$_2$] | 0.15 | 3 | 33 | >99 / >99* | 222 |
| 2 | [Pt(DMS)$_2$Cl$_2$] | 0.14 | 17 | 36 | >99 / >99* | 42 |
| 3 | [Pt(DMS)$_2$Cl$_2$] | 0.01 | 15 | 39 | >99 / >99* | 667 |
| 4 | [Pt(IMes)(DMS)Cl$_2$] | 0.13 | 14 | 36 | NR | / |
| 5 | [Pt(ICy)(DMS)Cl$_2$] | 1.00 | 21 | 70 | >99 / 36* | 5 |

*The reaction was also checked by ^{1}H NMR after 2 hours*

*Table 4: next five reactions suggested by the algorithm.*

| Entry | Catalyst | Cat. Loading (mol%) | Time (h) | T (°C) | Conversion (%) | TOF |
|-------|----------|---------------------|----------|--------|----------------|-----|
| 1 | [Pt(DMS)$_2$Cl$_2$] | 0.03 | 20 | 38 | 83 | 138 |
| 2 | [Pt(DMS)$_2$Cl$_2$] | 0.05 | 20 | 39 | >99* | 100 |
| 3 | [Pt(DMS)$_2$Cl$_2$] | 0.03 | 16 | 50 | 46 | 96 |
| 4 | [Pt(ICy)(DMS)Cl$_2$] | 0.01 | 18 | 70 | NR | / |
| 5 | [Pt(THT)$_2$Cl$_2$] | 0.45 | 14 | 37 | >99* | 16 |

*\* The reaction was already at >99% of conversion after 1 hour*

Along with the algorithm's recommendations, we chose to run some reactions without following Sunthetics' suggestions to further examine the system and see if the algorithm might overlook some considerations. In this regard, nine reactions based on chemical reasoning were conducted, including cases conducted at room temperature, a condition so far not recommended by the algorithm. The results of these experiments are shown in Table 5. All the reactions were sampled after 1, 2, 4, 6, 8, and 24 hours.

*Table 5: six reactions <u>not</u> suggested by the algorithm.*

| Entry | Catalyst | Cat. Loading (mol%) | T(°C) | Conversion (%) | | | | | | TOF* |
|-------|----------|---------------------|-------|-----|-----|-----|-----|-----|-----|------|
| | | | | 1h | 2h | 4h | 6h | 8h | 24h | |
| 1 | [Pt(DMS)$_2$Cl$_2$] | 0.13 | RT | **92** | 94 | 95 | 96 | 97 | **>99** | 32 |
| 2 | [Pt(IMes)(DMS)Cl$_2$] | 0.40 | 70 | 22 | 26 | 29 | 32 | 34 | 45 | 5 |
| 3 | [Pt(ICy)(DMS)Cl$_2$] | 0.40 | 50 | 19 | 22 | 36 | 44 | 49 | >99 | 10 |
| 4 | [Pt(DMS)$_2$Cl$_2$] | 0.03 | RT | 44 | 45 | 46 | 50 | 51 | 54 | 75 |
| 5 | [Pt(DMS)$_2$Cl$_2$] | 0.05 | RT | 20 | 26 | 29 | 33 | 36 | 38 | 32 |
| 6 | [Pt(THT)$_2$Cl$_2$] | 0.45 | RT | **>99** | - | - | - | - | >99 | 9 |

*Calculated after 24h*

Upon communicating these results to the algorithm, it generated various final outputs. In Figure 4 are shown the experiments in the reaction space. The graphical representation consists of a three-dimensional plot where the axes represent three variables: Conversion, Temperature, and Reaction Time. This graphical depiction facilitates a quick visual assessment of the regions, and hence the values of the variables, conducive to achieving higher conversions. Indeed, areas with maximized conversion (value of 1) are indicated by yellow dots. The same is shown also for the TON and the TOF in Figure 4.
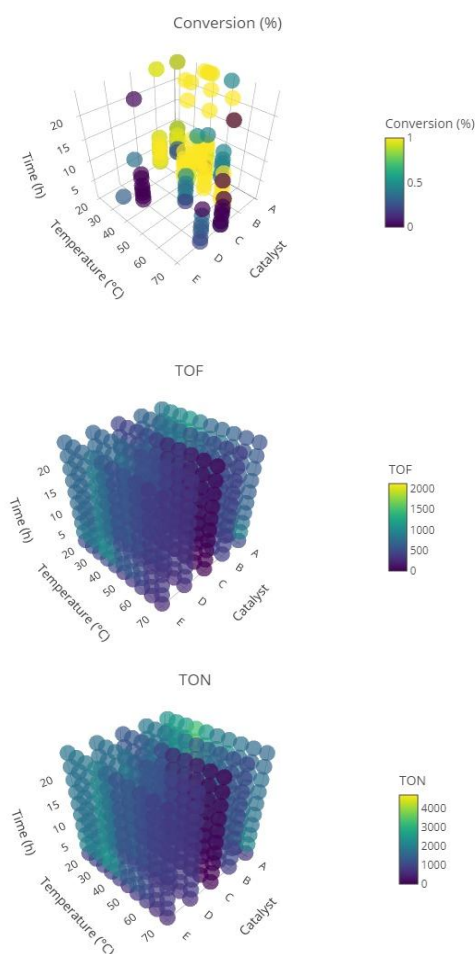
*Figure 4: three dimensional plots to visualize the conditions that maximize Conversion, TOF and TON. Catalyst A = [Pt(DMS)$_2$Cl$_2$], B = [Pt(THT)$_2$Cl$_2$], C = [Pt(ICy)DMS Cl$_2$], D = [Pt(IMes)DMSCl$_2$] and E = [Pt(SIPr)DMS Cl$_2$].*

In Figure 5 is reported the variable importance in descending order, with the most important variable at the top for the three targets: the TON, the Conversion (%) and the TOF, so it is easy to see the parameters that are affecting the system the most. From the analysis of the plot, it is evident that the most critical variable concerning the maximization of the TON is the reaction time. Immediately following with a slightly lower value is the catalyst loading, which thus holds a similar significance. For the Conversion, the catalyst choice is of utmost importance, while for the TOF, the most crucial factor is the catalyst loading.
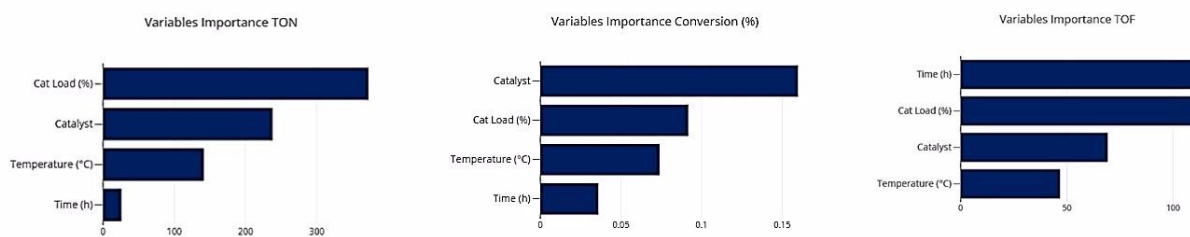
*Figure 5: variable importance for the three targets of the reaction: TON, TOF and Conversion (%).*

After that, the prediction error was calculated, and it is reported in Figure 6. In the graph the x-axis representing the observed value and the y-axis representing the obtained value. It is an illustration about the relationship between observed values and corresponding obtained ones. Upon examining the distribution of obtained values, it is evident that they closely align with the trendline drawn by the predicted values. This observation suggests a strong correlation, indicative of a well-functioning model.
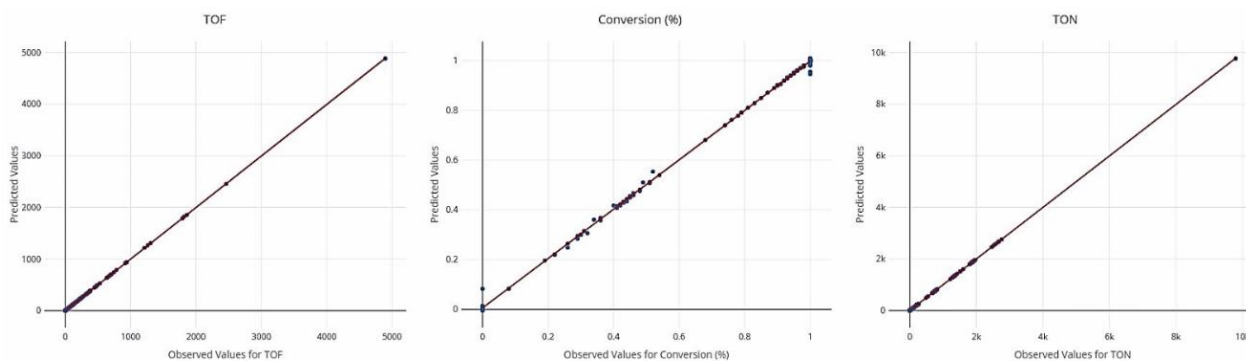


*Figure 6: prediction error: deviation between the anticipated values of TOF, Conversion, and TON and the experimentally acquired values.*

## *Conclusion Project 2*

Interpreting the values obtained from the initial analyses reported in Table 1, it can be immediately inferred that [Pt(DMS)$_2$Cl$_2$] and [Pt(THT)$_2$Cl$_2$] appear to be the superior catalysts for this reaction for now. Indeed, among the first ten reactions suggested by the algorithm, the one in which [Pt(DMS)$_2$Cl$_2$] (0.15 mol%) was employed as the catalyst at a temperature of 34 °C exhibited the highest performance (see entry 6 Table 1), with a total conversion after 3 hours and a high TOF value (222). In general, a higher value of TOF may indicate better catalytic performance; however, it is not the only factor to consider. The TOF denotes the number of reactions catalyzed by a single molecule of catalyst within a given period. Nevertheless, other factors such as catalyst selectivity (the ability to produce only the desired product), catalyst stability over time, and its economic feasibility must also be considered. In some cases, a catalyst may exhibit a very high TOF but could be unstable or selectively inefficient. Conversely, a catalyst with a slightly lower TOF may be more stable over time and more selective, ultimately rendering it more effective in an industrial or laboratory process.

Another highly promising result emerged from the initial tests, as shown in Table 1 entry 10: the reaction employing [Pt(THT)$_2$Cl$_2$] (0.50 mol%) led to complete substrate conversion within 20 hours at 50 °C. In the subsequent five reactions conducted, whose outcomes are reported in Table 5, the best performances were again achieved using [Pt(DMS)$_2$Cl$_2$] as the catalyst. Despite the algorithm suggesting a reaction time among other variables, reactions were also tested after a common duration of 2 hours to provide further monitoring of reaction progress. This led to interesting results; for example, examining the conversions of the first three entries in Table 3 reveals that complete conversion was achieved even after 2 hours, despite the algorithm suggesting waiting periods of 3, 17, and 15 hours, respectively. In the first set of reactions, the Pt(II)-ICy-based catalyst yielded a 48% conversion after 2 hours of reaction (see entry 3 in Table 1), even if with maximum catalyst quantity (1 mol%). Then, in the second set of reactions, the algorithm suggested repeating the trial but increasing the temperature from 50 to 70 °C and waiting for 21 hours instead of 2 (see entry 5 Table 3). The result was complete conversion, yet it cannot be considered optimal due to the low TOF value (5), high catalyst quantity, elevated temperature, and reaction duration. This is a clear example of how it is crucial to consider all aspects comprehensively, seeking the best combination that yields

maximum results with minimal effort when optimizing a reaction. The best result was obtained with the [Pt(DMS)$_2$Cl$_2$] (0.01 mol%) at 39 °C in 2 hours (see entry 3 Table 3), in fact the conversion was complete already after 2 hours and the value of the TOF is 4,950 that is the highest obtained. In the subsequent third set of reactions, as detailed in Table 4, two reactions were attempted with very low quantities of [Pt(DMS)$_2$Cl$_2$] catalyst. Once it was established that this catalyst performed well, it made sense to try to minimize the required quantity. Entry 2 in Table 4 illustrates how a mere 0.05 mol% of [Pt(DMS)$_2$Cl$_2$] was sufficient to achieve complete conversion after one hour of reaction at 39 °C . Another interesting result is seen in entry 5 of Table 4: the reaction employing [Pt(THT)$_2$Cl$_2$] at 0.45 mol% at 37 °C resulted in complete conversion after one hour. Between the two catalysts, despite both being very fast and efficient, [Pt(DMS)$_2$Cl$_2$] allows achieving similar results with much lower quantities, making it the optimal choice for reaction optimization. Throughout the project, in addition to the reactions suggested by the algorithm, some reactions not recommended by it were also conducted. As the results of the previous reactions became available, considerations were made, and reaction conditions were devised accordingly. These reactions executed without the aid of the algorithm are presented in Table 5. Two reactions are particularly noteworthy: the first one (see entry 1) employing [Pt(DMS)$_2$Cl$_2$] 0.13 mol% at room temperature and the one reported in entry 6 using [Pt(THT)$_2$Cl$_2$] at 0.45 mol% at room temperature too. Analyzing the results, it is evident that in the first reaction, substrate conversion reached 92% after just one hour, followed by a slowdown until complete conversion was achieved after 24 hours. As for the reaction with [Pt(THT)$_2$Cl$_2$], complete conversion was observed after one hour, primarily due to the significantly higher catalyst quantity compared to the other considered reaction. In conclusion, it was determined that the optimal combination for this reaction is either [Pt(DMS)$_2$Cl$_2$] at 0.05 mol% and 0.01 mol% at 40 °C or [Pt(THT)$_2$Cl$_2$] at 0.40 mol% at room temperature. The algorithm proved to be highly beneficial for optimization purposes, accelerating the process and utilizing less material than would have been used otherwise. It is a highly intriguing approach that, when coupled with operator expertise, can yield significant results, even in more complex reactions with multiple variables to parameterize.

The reaction was tested on a single simple substrate to facilitate its optimization, but expanding its application in the future to other substrates would be highly intriguing. Figure 8 presents a potential scope of various amides that could be utilized as future substrates to apply the optimized reduction reaction. For future developments, it would be interesting to explore the possibility of changing the

silane utilized in the reaction, assessing whether its efficacy improves. This could involve investigating the utilization of industrial by-products or economically viable materials to determine their potential benefits.

N,N-dimethylbenzamide

N,N-dibenzyl-2-cyanoacetamide

N,N-diethyl-3-methylbenzamide

N-(2-aminoethyl)acetamide

N-(furan-2-ylmethyl)-3-methylbenzamide

N-(4-hydroxyphenyl)acetamide

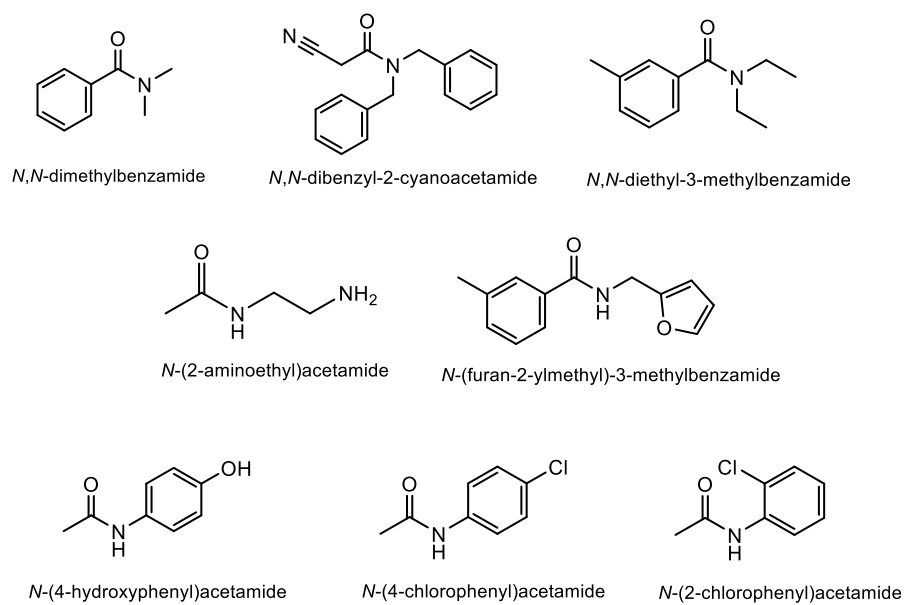N-(4-chlorophenyl)acetamide

N-(2-chlorophenyl)acetamide

*Figure 8: Scope for the future reactions.*

# *References*

[1]   H. V. Huynh, *The Organometallic Chemistry of N-Heterocyclic Carbenes*, John Wiley & Sons, **2017**.

[2]   A. J. I. Arduengo, R. L. Harlow, M. Kline, *J. Am. Chem. Soc.* **1991**, *113*, 361–363.

[3]   A. D. McNaught, A. Wilkinson, *Compendium of Chemical Terminology*, Blackwell Science Oxford, **1997**.

[4]   X. Shang, C. Yang, S. L. Morris-Natschke, J. Li, X. Yin, Y. Liu, X. Guo, J. Peng, M. Goto, J. Zhang, *Med. Res. Rev.* **2020**, *40*, 2212–2289.

[5]   W. A. Herrmann, *Angew. Chem. Int. Ed.* **2002**, *41*, 1290–1309.

[6]   X. Ma, M. V. Mane, L. Cavallo, S. P. Nolan, *Eur. J. Org. Chem.* **2023**, *26*, e202201466.

[7]   D. Bourissou, O. Guerret, F. P. Gabbaï, G. Bertrand, *Chem. Rev.* **2000**, *100*, 39–92.

[8]   S. De, A. Udvardy, C. E. Czégéni, F. Joo, *Coord. Chem. Rev.* **2019**, *400*, 213038.

[9]   H. W. Wanzlick, *Angew. Chem. Int. Ed. Engl.* **1962**, *1*, 75–80.

[10]  H. Wanzlick, H. Schönherr, *Angew. Chem. Int. Ed. Engl.* **1968**, *7*, 141–142.

[11]  A. J. Arduengo III, R. L. Harlow, M. Kline, *J. Am. Chem. Soc.* **1991**, *113*, 361–363.

[12]  S. Diez-Gonzalez, N. Marion, S. P. Nolan, *Chem. Rev.* **2009**, *109*, 3612–3676.

[13]  K. Öfele, W. A. Herrmann, D. Mihalios, M. Elison, E. Herdtweck, W. Scherer, J. Mink, *J. Organomet. Chem.* **1993**, *459*, 177–184.

[14]  W. A. Herrmann, C. Köcher, *Angew. Chem. Int. Ed. Engl.* **1997**, *36*, 2162–2187.

[15]  M. N. Hopkinson, C. Richter, M. Schedler, F. Glorius, *Nature* **2014**, *510*, 485–496.

[16] F. Cuccu, L. De Luca, F. Delogu, E. Colacino, N. Solin, R. Mocci, A. Porcheddu, *ChemSusChem* **2022**, *15*, e202200362.

[17] S. P. Nolan, *N-Heterocyclic Carbenes: Effective Tools for Organometallic Synthesis*, John Wiley & Sons, **2014**.

[18] O. Briel, C. S. Cazin, *N-Heterocycl. Carbenes Transit. Met. Catal. Organocatalysis* **2011**, 315–324.

[19] R. R. Schrock, *Angew. Chem. Int. Ed.* **2006**, *45*, 3748–3759.

[20] P. De Fremont, N. Marion, S. P. Nolan, *Coord. Chem. Rev.* **2009**, *253*, 862–892.

[21] N. Mirzadeh, T. S. Reddy, S. K. Bhargava, *Coord. Chem. Rev.* **2019**, *388*, 343–359.

[22] A. A. Tulloch, A. A. Danopoulos, S. Winston, S. Kleinhenz, G. Eastham, *J. Chem. Soc. Dalton Trans.* **2000**, 4499–4506.

[23] T. A. C. A. Bayrakdar, F. Nahra, J. V. Davis, M. M. Gamage, B. Captain, M. Temprado, M. Marazzi, M. Saab, K. V. Hecke, D. Ormerod, C. D. Hoff, S. P. Nolan, *Organometallics* **2020**, *39*, 2907–2916.

[24] D. Bourissou, O. Guerret, *Chem Rev* **1999**, *100*, 39–92.

[25] C. Heinemann, T. Müller, Y. Apeloig, H. Schwarz, *J. Am. Chem. Soc.* **1996**, *118*, 2023–2038.

[26] P. De Fremont, N. Marion, S. P. Nolan, *Coord. Chem. Rev.* **2009**, *253*, 862–892.

[27] H. Buhl, C. Ganter, *Chem. Commun.* **2013**, *49*, 5417–5419.

[28] M. C. Jahnke, F. E. Hahn, *Transit. Met. Complexes Neutral Eta1-Carbon Ligands* **2010**, 95–129.

[29] X. Bantreil, S. P. Nolan, *Nat. Protoc.* **2011**, *6*, 69–77.

[30] M. Hans, J. Lorkowski, A. Demonceau, L. Delaude, *Beilstein J. Org. Chem.* **2015**, *11*, 2318–2325.

[31] T. Dröge, F. Glorius, *Angew. Chem. Int. Ed.* **2010**, *49*, 6940–6952.

[32] D. I. Bezuidenhout, S. Lotz, D. C. Liles, B. van der Westhuizen, *Recent Dev. Organomet. Chem. 2012* **2012**, *256*, 479–524.

[33] M. Stradiotto, R. J. Lundgren, *Ligand Design in Metal Chemistry*, Wiley Online Library, **2016**.

[34] D. J. Durand, N. Fey, *Chem. Rev.* **2019**, *119*, 6561–6594.

[35] C. A. Tolman, *Chem. Rev.* **1977**, *77*, 313–348.

[36] C. A. Tolman, *Chem. Rev.* **1977**, *77*, 313–348.

[37] H. Clavier, S. P. Nolan, *Chem. Commun.* **2010**, *46*, 841–861.

[38] G. Berthon-Gelloz, O. Buisine, J.-F. Brière, G. Michaud, S. Stérin, G. Mignani, B. Tinant, J.-P. De-clercq, D. Chapon, I. E. Markó, *J. Organomet. Chem.* **2005**, *690*, 6156–6168.

[39] A. C. Hillier, W. J. Sommer, B. S. Yong, J. L. Petersen, L. Cavallo, S. P. Nolan, *Organometallics* **2003**, *22*, 4322–4326.

[40] A. Poater, F. Ragone, R. Mariz, R. Dorta, L. Cavallo, *Chem. Eur. J.* **2010**, *16*, 14348–14353.

[41] A. Gómez-Suárez, D. J. Nelson, S. P. Nolan, *Chem. Commun.* **2017**, *53*, 2650–2660.

[42] D. Cremer, E. Kraka, *Dalton Trans.* **2017**, *46*, 8323–8338.

[43] R. Dorta, E. D. Stevens, N. M. Scott, C. Costabile, L. Cavallo, C. D. Hoff, S. P. Nolan, *J. Am. Chem. Soc.* **2005**, *127*, 2485–2495.

[44] R. Dorta, E. D. Stevens, C. D. Hoff, S. P. Nolan, *J. Am. Chem. Soc.* **2003**, *125*, 10490–10491.

[45] A. R. Chianese, X. Li, M. C. Janzen, J. Faller, R. H. Crabtree, *Organometallics* **2003**, *22*, 1663–1667.

[46] R. A. Kelly Iii, H. Clavier, S. Giudice, N. M. Scott, E. D. Stevens, J. Bordner, I. Samardjiev, C. D. Hoff, L. Cavallo, S. P. Nolan, *Organometallics* **2008**, *27*, 202–210.

[47] S. Wolf, H. Plenio, *J. Organomet. Chem.* **2009**, *694*, 1487–1492.

[48] C. S. Cazin, *N-Heterocyclic Carbenes in Transition Metal Catalysis and Organocatalysis*, Springer Science & Business Media, **2010**.

[49] T. Scattolin, S. P. Nolan, *Trends Chem.* **2020**, *2*, 721–736.

[50] H. M. Wang, I. J. Lin, *Organometallics* **1998**, *17*, 972–975.

[51]  M. R. Furst, C. S. Cazin, *Chem. Commun.* **2010**, *46*, 6924–6925.

[52]  R. Visbal, M. C. Gimeno, *Chem. Soc. Rev.* **2014**, *43*, 3551–3574.

[53]  E. A. Martynova, N. V. Tzouras, G. Pisanò, C. S. Cazin, S. P. Nolan, *Chem. Commun.* **2021**, *57*, 3836–3856.

[54]  J. F. Hartwig, J. P. Collman, *Organotransition Metal Chemistry: From Bonding to Catalysis*, Springer, **2010**.

[55]  B. P. Maliszewski, T. A. Bayrakdar, P. Lambert, L. Hamdouna, X. Trivelli, L. Cavallo, A. Poater, M. Beliš, O. Lafon, K. Van Hecke, *Chem. Eur. J.* **2023**, *29*, e202301259.

[56]  B. Marciniec, *Tarrytown N. Y.* **1992**.

[57]  J. V. Obligacion, P. J. Chirik, *Nat. Rev. Chem.* **2018**, *2*, 15–34.

[58]  J. L. Speier, J. A. Webster, G. H. Barnes, *J. Am. Chem. Soc.* **1957**, *79*, 974–979.

[59]  H. Bai, *Ind. Eng. Chem. Res.* **2012**, *51*, 16457–16466.

[60]  G. De Bo, G. Berthon-Gelloz, B. Tinant, I. E. Markó, *Organometallics* **2006**, *25*, 1881–1890.

[61]  S. Hanada, E. Tsutsumi, Y. Motoyama, H. Nagashima, *J. Am. Chem. Soc.* **2009**, *131*, 15032–15040.

[62]  B. Marciniec, *Coord. Chem. Rev.* **2005**, *249*, 2374–2390.

[63]  L. Sommer, E. Pietrusza, F. Whitmore, *J. Am. Chem. Soc.* **1947**, *69*, 188–188.

[64]  B. Karstedt, *US Pat. US3775452A* **1973**.

[65]  M. F. Lappert, F. P. Scott, *J. Organomet. Chem.* **1995**, *492*, C11–C13.

[66]  L. D. de Almeida, H. Wang, K. Junge, X. Cui, M. Beller, *Angew. Chem. Int. Ed.* **2021**, *60*, 550–565.

[67]  I. E. Marko, S. Sterin, O. Buisine, G. Mignani, P. Branlard, B. Tinant, J.-P. Declercq, *Science* **2002**, *298*, 204–206.

[68] T. A. C. A. Bayrakdar, B. P. Maliszewski, F. Nahra, D. Ormerod, S. P. Nolan, *ChemSusChem* **2021**, *14*, 3810–3814.

[69] S. Hanada, E. Tsutsumi, Y. Motoyama, H. Nagashima, *J. Am. Chem. Soc.* **2009**, *131*, 15032–15040.

[70] D. Troegel, J. Stohrer, *Coord. Chem. Rev.* **2011**, *255*, 1440–1459.

[71] Y. Nakajima, S. Shimada, *RSC Adv.* **2015**, *5*, 20603–20616.

[72] S. Sakaki, N. Mizoe, M. Sugimoto, *Organometallics* **1998**, *17*, 2510–2523.

[73] B. P. Maliszewski, E. Casillo, P. Lambert, F. Nahra, C. S. Cazin, S. P. Nolan, *Chem. Commun.* **2023**, *59*, 14017–14020.

[74] J. Ammer, H. Mayr, *J. Phys. Org. Chem.* **2013**, *26*, 59–63.

[75] I. Colomer, A. E. R. Chamberlain, M. B. Haughey, T. J. Donohoe, *Nat. Rev. Chem.* **2017**, *1*, 0088.

[76] N. V. Tzouras, L. P. Zorba, E. Kaplanai, N. Tsoureas, D. J. Nelson, S. P. Nolan, G. C. Vougioukalakis, *ACS Catal.* **2023**, *13*, 8845–8860.

[77] X. An, J. Xiao, *Chem. Rec.* **2020**, *20*, 142–161.

[78] K. Neimann, R. Neumann, *Org. Lett.* **2000**, *2*, 2861–2863.

[79] A. Berkessel, M. R. Andreae, *Tetrahedron Lett.* **2001**, *42*, 2293–2295.

[80] H. F. Motiwala, M. Charaschanya, V. W. Day, J. Aube, *J. Org. Chem.* **2016**, *81*, 1593–1609.

[81] R. H. Vekariya, J. Aube, *Org. Lett.* **2016**, *18*, 3534–3537.

[82] M. O. Ratnikov, V. V. Tumanov, W. A. Smit, *Angew. Chem.* **2008**, *120*, 9885–9888.

[83] J. M. Ramos-Villaseñor, E. Rodríguez-Cárdenas, C. E. Barrera Díaz, B. A. Frontana-Uribe, *J. Electrochem. Soc.* **2020**, *167*, 155509.

[84] S. Dierick, E. Vercruysse, G. Berthon-Gelloz, I. E. Markó, *Chem. Eur. J.* **2015**, *21*, 17073–17078.

[85] J. Coetzee, D. L. Dodds, J. Klankermayer, S. Brosinski, W. Leitner, A. M. Slawin, D. J. Cole-Hamilton, *Chem. Eur. J.* **2013**, *19*, 11039–11050.

[86] D. Matheau-Raven, P. Gabriel, J. A. Leitch, Y. A. Almehmadi, K. Yamazaki, D. J. Dixon, *ACS Catal.* **2020**, *10*, 8880–8897.

[87] V. Froidevaux, C. Negrell, S. Caillol, J.-P. Pascault, B. Boutevin, *Chem. Rev.* **2016**, *116*, 14181–14224.

[88] A. Trowbridge, S. M. Walton, M. J. Gaunt, *Chem. Rev.* **2020**, *120*, 2613–2692.

[89] J. A. Leitch, T. Rossolini, T. Rogova, J. A. P. Maitland, D. J. Dixon, *ACS Catal.* **2020**, *10*, 2009–2025.

[90] M. Gibson, R. Bradshaw, *Angew. Chem. Int. Ed. Engl.* **1968**, *7*, 919–930.

[91] S. Lang, J. Murphy, *Chem. Soc. Rev.* **2006**, *35*, 146–156.

[92] J. Song, Z.-F. Huang, L. Pan, K. Li, X. Zhang, L. Wang, J.-J. Zou, *Appl. Catal. B Environ.* **2018**, *227*, 386–408.

[93] H. Staudinger, J. Meyer, *Helv. Chim. Acta* **1919**, *2*, 635–646.

[94] G. Arnott, **2014**.

[95] W. G. Nigh, *J. Chem. Educ.* **1975**, *52*, 670.

[96] A. Murray, L. Williams, *Organic Syntheses with Isotopes*, Interscience Publishers, **1958**.

[97] E. Nyfeler, P. Renaud, *Chimia* **2006**, *60*, 276–276.

[98] H. Wolff, *Org. React.* **2004**, *3*, 307–336.

[99] A. W. Hofmann, *Berichte Dtsch. Chem. Ges.* **1881**, *14*, 2725–2736.

[100] E. S. Wallis, J. F. Lane, in *Org. React.*, John Wiley & Sons, Ltd, **2011**, pp. 267–306.

[101] T. Shioiri, in *Compr. Org. Synth.* (Eds.: B.M. Trost, I. Fleming), Pergamon, Oxford, **1991**, pp. 795–828.

[102] J. Volf, J. Pašek, in *Stud. Surf. Sci. Catal.*, Elsevier, **1986**, pp. 105–144.

[103] H. Elsen, J. Langer, G. Ballmann, M. Wiesinger, S. Harder, *Chem. Eur. J.* **2021**, *27*, 401–411.

[104] A. Pavlic, H. Adkins, *J. Am. Chem. Soc.* **1946**, *68*, 1471–1471.

[105] J. Margitfalvi, L. Guczi, A. H. Weiss, *J. Catal.* **1981**, *72*, 185–198.

[106] B. Ohtani, S. Takamiya, Y. Hirai, M. Sudoh, S. Nishimoto, T. Kagiya, *J. Chem. Soc. Perkin Trans. 2* **1992**, 175–179.

[107] Y. G. Gololobov, L. F. Kasukhin, *Tetrahedron* **1992**, *48*, 1353–1406.

[108] A. F. Abdel-Magid, K. G. Carson, B. D. Harris, C. A. Maryanoff, R. D. Shah, *J. Org. Chem.* **1996**, *61*, 3849–3862.

[109] M. Delépine, *Bull Soc Chim Fr. 3* **1895**, *13*, 352–361.

[110] K. A. Schellenberg, *J. Org. Chem.* **1963**, *28*, 3259–3261.

[111] W. S. Emerson, *Org. React.* **2004**, *4*, 174–255.

[112] F. F. Blicke, J. H. Burckhalter, *J. Am. Chem. Soc.* **1942**, *64*, 451–454.

[113] M. Kitamura, D. Lee, S. Hayashi, S. Tanaka, M. Yoshimura, *J. Org. Chem.* **2002**, *67*, 8685–8687.

[114] K. Ito, H. Oba, M. Sekiya, *Bull. Chem. Soc. Jpn.* **1976**, *49*, 2485–2490.

[115] Q. Umar, M. Luo, *Reactions* **2023**, *4*, 117–147.

[116] S. Gomez, J. A. Peters, T. Maschmeyer, *Adv. Synth. Catal.* **2002**, *344*, 1037–1057.

[117] C. L. Barney, E. V. Huber, J. R. McCarthy, *Tetrahedron Lett.* **1990**, *31*, 5547–5550.

[118] E. Vitaku, D. T. Smith, J. T. Njardarson, *J. Med. Chem.* **2014**, *57*, 10257–10274.

[119] U. Scholz, *ChemInform* **2009**, *40*, i.

[120] P. A. Forero-Cortés, A. M. Haydl, *Org. Process Res. Dev.* **2019**, *23*, 1478–1483.

[121] K. J. Koroluk, D. A. Jackson, A. P. Dicks, *J. Chem. Educ.* **2012**, *89*, 796–798.

[122] K. O. Biriukov, E. Podyacheva, I. Tarabrin, O. I. Afanasyev, D. Chusov, *J. Org. Chem.* **2024**, *89*, 3580–3584.

[123] S. H. Pine, *J. Chem. Educ.* **1968**, *45*, 118.

[124] H. Brunner, W. Miehling, *J. Organomet. Chem.* **1984**, *275*, c17–c21.

[125] D. C. Apple, K. A. Brady, J. M. Chance, N. E. Heard, T. A. Nile, *J. Mol. Catal.* **1985**, *29*, 55–64.

[126] T. Schmidt, *Tetrahedron Lett.* **1994**, *35*, 3513–3516.

[127] I. Ojima, M. Nihonyanagi, Y. Nagai, *J Chem Soc Chem Commun* **1972**, 938a–938a.

[128] C. Eaborn, K. Odell, A. Pidcock, *J. Organomet. Chem.* **1973**, *63*, 93–97.

[129] T. Nakano, Y. Nagai, *Chem. Lett.* **1988**, *17*, 481–484.

[130] T. Ohkuma, S. Hashiguchi, R. Noyori, *J. Org. Chem.* **1994**, *59*, 217–221.

[131] L. Vaska, J. W. DiLuzio, *J. Am. Chem. Soc.* **1961**, *83*, 2784–2785.

[132] H. Nishiyama, K. Itoh, *Catal. Asymmetric Synth.* **2000**, *2*, 267–88.

[133] H. C. Brown, P. Heim, *J. Am. Chem. Soc.* **1964**, *86*, 3566–3567.

[134] L. Pasumansky, C. T. Goralski, B. Singaram, *Org. Process Res. Dev.* **2006**, *10*, 959–970.

[135] J. Magano, J. R. Dunetz, *Org. Process Res. Dev.* **2012**, *16*, 1156–1184.

[136] C. W. Lee, H. M. Ko, *Asian J. Org. Chem.* **2023**, e202300098.

[137] A. E. Finholt, A. C. Jr. Bond, H. I. Schlesinger, *J. Am. Chem. Soc.* **1947**, *69*, 1199–1203.

[138] H. I. Schlesinger, H. C. Brown, A. E. Finholt, *J. Am. Chem. Soc.* **1953**, *75*, 205–209.

[139] J. R. Cabrero-Antonino, R. Adam, V. Papa, M. Beller, *Nat. Commun.* **2020**, *11*, 3893.

[140] V. Vinayagam, S. K. Sadhukhan, S. K. Karre, R. Srinath, R. K. Maroju, P. R. Karra, H. S. N. B. Bathula, S. Kundrapu, S. R. Surukonti, *Org. Lett.* **2023**.

[141] S. Bower, K. A. Kreutzer, S. L. Buchwald, *Angew. Chem. Int. Ed. Engl.* **1996**, *35*, 1515–1516.

[142] K. Selvakumar, K. Rangareddy, J. F. Harrod, *Can. J. Chem.* **2004**, *82*, 1244–1248.

[143] R. Kuwano, M. Takahashi, Y. Ito, *Tetrahedron Lett.* **1998**, *39*, 1017–1020.

[144] M. Igarashi, T. Fuchikami, *Tetrahedron Lett.* **2001**, *42*, 1945–1947.

[145] A. C. Fernandes, C. C. Romão, *J. Mol. Catal. Chem.* **2007**, *272*, 60–63.

[146] S. Hanada, T. Ishida, Y. Motoyama, H. Nagashima, *J. Org. Chem.* **2007**, *72*, 7551–7559.

[147] S. Das, D. Addis, S. Zhou, K. Junge, M. Beller, *J. Am. Chem. Soc.* **2010**, *132*, 1770–1771.

[148] C. M. Kelly, R. McDonald, O. L. Sydora, M. Stradiotto, L. Turculet, *Angew. Chem. Int. Ed.* **2017**, *56*, 15901–15904.

[149] C. Cheng, M. Brookhart, *J. Am. Chem. Soc.* **2012**, *134*, 11304–11307.

[150] M. Kobylarski, L. J. Donnelly, J.-C. Berthet, T. Cantat, *Green Chem.* **2022**, *24*, 6810–6815.

[151] B. J. Simmons, M. Hoffmann, J. Hwang, M. K. Jackl, N. K. Garg, *Org. Lett.* **2017**, *19*, 1910–1913.

[152] P.-Q. Huang, Q.-W. Lang, Y.-R. Wang, *J. Org. Chem.* **2016**, *81*, 4235–4243.

[153] G. Pelletier, W. S. Bechara, A. B. Charette, *J. Am. Chem. Soc.* **2010**, *132*, 12817–12819.

[154] W. Yao, H. Fang, Q. He, D. Peng, G. Liu, Z. Huang, *J. Org. Chem.* **2019**, *84*, 6084–6093.

[155] W. Yao, L. He, D. Han, A. Zhong, *J. Org. Chem.* **2019**, *84*, 14627–14635.

[156] D. Mukherjee, S. Shirase, K. Mashima, J. Okuda, *Angew. Chem. Int. Ed.* **2016**, *55*, 13326–13329.

[157] S. Das, D. Addis, L. R. Knöpke, U. Bentrup, K. Junge, A. Brückner, M. Beller, *Angew. Chem. Int. Ed.* **2011**, *39*, 9180–9184.

[158] Y. Li, J. A. Molina de La Torre, K. Grabow, U. Bentrup, K. Junge, S. Zhou, A. Brückner, M. Beller, *Angew. Chem. Int. Ed.* **2013**, *52*, 11577–11580.

[159] V. Vinayagam, T. V. Hajay Kumar, R. Nune, S. K. Karre, S. K. Sadhukhan, *J. Org. Chem.* **2023**, *88*, 2122–2131.

[160] N. Nakatani, J. Hasegawa, Y. Sunada, H. Nagashima, *Dalton Trans.* **2015**, *44*, 19344–19356.

[161] J. Pesti, G. L. Larson, *Org. Process Res. Dev.* **2016**, *20*, 1164–1181.

[162] H. Nagashima, K. Tatebe, T. Ishibashi, A. Nakaoka, J. Sakakibara, K. Itoh, *Organometallics* **1995**, *14*, 2868–2879.

[163] H. Nagashima, A. Suzuki, T. Iura, K. Ryu, K. Matsubara, *Organometallics* **2000**, *19*, 3579–3590.

[164] N. Artrith, K. T. Butler, F.-X. Coudert, S. Han, O. Isayev, A. Jain, A. Walsh, *Nat. Chem.* **2021**, *13*, 505–508.

[165] J. A. Keith, V. Vassilev-Galindo, B. Cheng, S. Chmiela, M. Gastegger, K.-R. Müller, A. Tkatchenko, *Chem. Rev.* **2021**, *121*, 9816–9872.

[166] T. M. Mitchell, *AI Mag.* **1997**, *18*, 11–11.

[167] M. Meuwly, *Chem. Rev.* **2021**, *121*, 10218–10239.

[168] T. M. Mitchell, **1997**.

[169] Y. LeCun, Y. Bengio, G. Hinton, *Nature* **2015**, *521*, 436–444.

[170] A. Binder, M. Bockmayr, M. Hägele, S. Wienert, D. Heim, K. Hellweg, M. Ishii, A. Stenzinger, A. Hocke, C. Denkert, *Nat. Mach. Intell.* **2021**, *3*, 355–366.

[171] P. Baldi, P. Sadowski, D. Whiteson, *Nat. Commun.* **2014**, *5*, 4308.

[172] T. Lengauer, O. Sander, S. Sierra, A. Thielen, R. Kaiser, *Nat. Biotechnol.* **2007**, *25*, 1407–1410.

[173] A. W. Senior, R. Evans, J. Jumper, J. Kirkpatrick, L. Sifre, T. Green, C. Qin, A. Žídek, A. W. Nelson, A. Bridgland, *Nature* **2020**, *577*, 706–710.

[174] B. Blankertz, R. Tomioka, S. Lemm, M. Kawanabe, K.-R. Muller, *IEEE Signal Process. Mag.* **2007**, *25*, 41–56.

[175] D. Ferrucci, A. Levas, S. Bagchi, D. Gondek, E. T. Mueller, *Artif. Intell.* **2013**, *199*, 93–105.

[176] D.-O. Won, K.-R. Müller, S.-W. Lee, *Sci. Robot.* **2020**, *5*, eabb9764.

[177] Y. Motoyama, M. Aoki, N. Takaoka, R. Aoto, H. Nagashima, *Chem. Commun.* **2009**, 1574–1576.

[178] V. Vapnik, *The Nature of Statistical Learning Theory*, Springer Science & Business Media, **1999**.

[179] "Sunthetics - Accelerating innovation in the chemical industry with AI," can be found under https://sunthetics.io/, **n.d.**

[180] A. J. Surman, M. Rodriguez-Garcia, Y. M. Abul-Haija, G. J. T. Cooper, P. S. Gromski, R. Turk-Mac-Leod, M. Mullin, C. Mathis, S. I. Walker, L. Cronin, *Proc. Natl. Acad. Sci.* **2019**, *116*, 5387–5392.

[181] R. Dybowski, *New J Chem* **2020**, *44*, 20914–20920.

[182] M. Boudart, A. Aldag, J. E. Benson, N. A. Dougharty, C. G. Harkins, *J. Catal.* **1966**, *6*, 92–99.

[183] *Pure Appl. Chem.* **1976**, *46*, 71–90.

[184] S. Kozuch, J. M. L. Martin, *ACS Catal.* **2012**, *2*, 2787–2794.

[185] **2019**, DOI doi:10.1351/goldbook.T06534.

[186] V. Leskovac, *Comprehensive Enzyme Kinetics*, Springer Science & Business Media, **2003**.

[187] G. Rothenberg, *Catalysis: Concepts and Green Applications*, John Wiley & Sons, **2017**.

[188] T. A. Rogers, A. S. Bommarius, *Chem. Eng. Sci.* **2010**, *65*, 2118–2124.

[189] D. Chicco, M. J. Warrens, G. Jurman, *PeerJ Comput. Sci.* **2021**, *7*, e623.

[190] D. Didona, P. Romano, **2014**, DOI 10.48550/arXiv.1410.5102.

# *Appendix*

This is a collection of some representative spectra obtained in the laboratory.
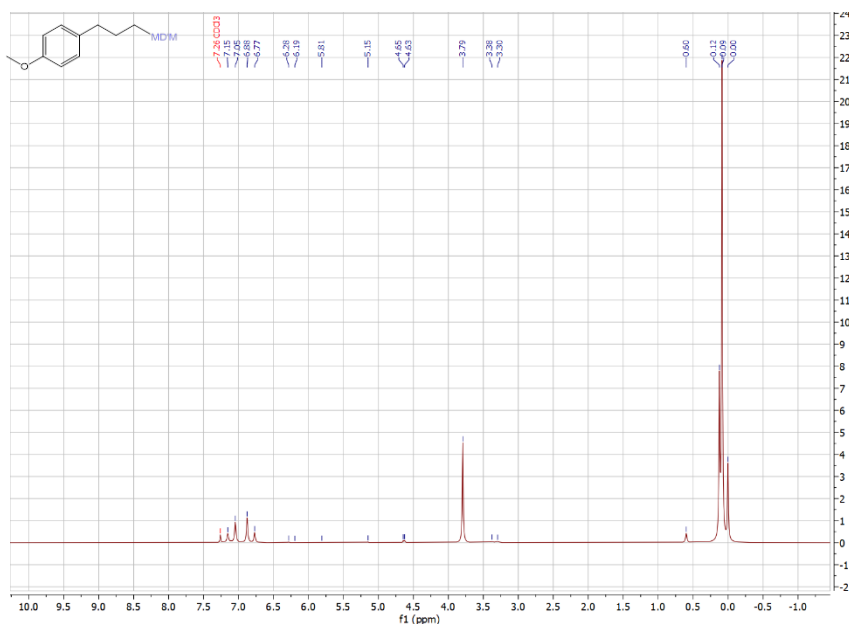


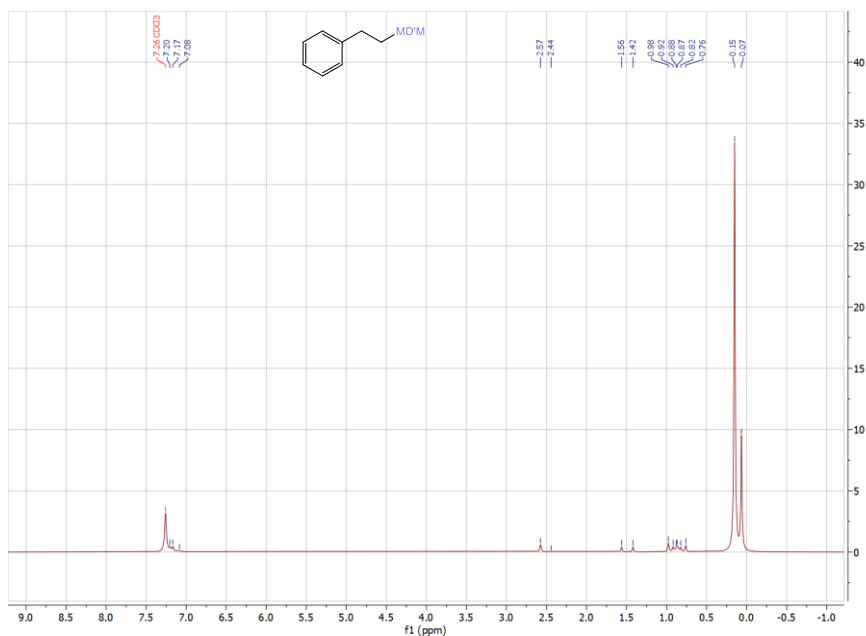*Figure A1: 1H NMR (80 MHz, CDCl3, 298K) of substrate number 4 Chapter "1.4 Substrates scope".*



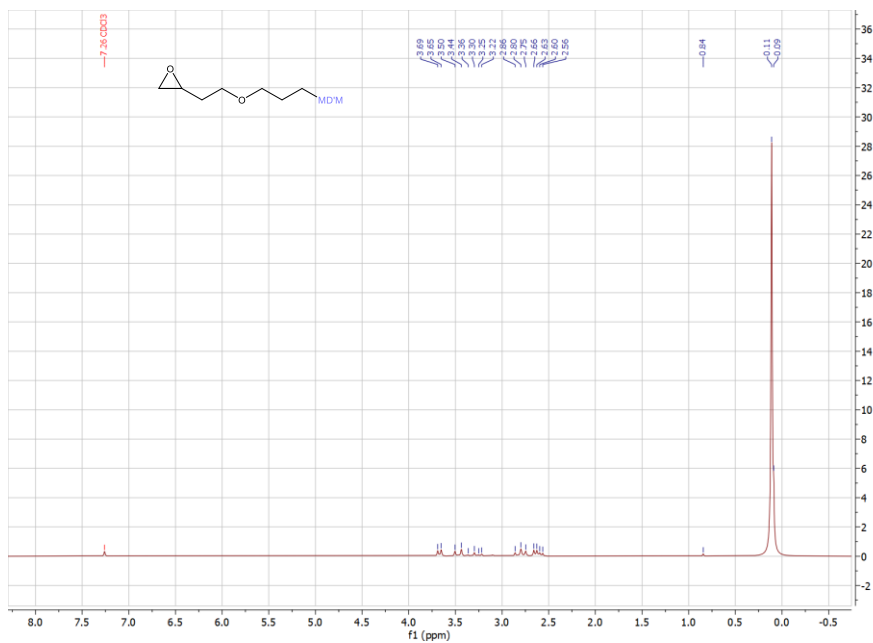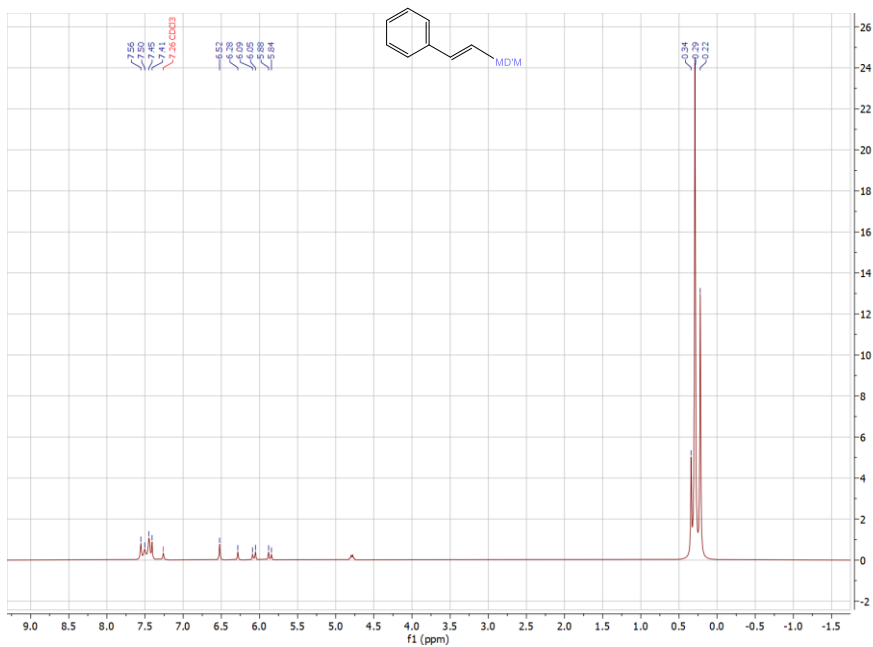*Figure A2: ¹H NMR (80 MHz, CDCl3, 298K) of of substrate number 3 Chapter "1.4 Substrates scope".*

*Figure A3: $^1$H NMR (80 MHz, CDCl3, 298K) of substrate number **7** Chapter "1.4 Substrates scope".*
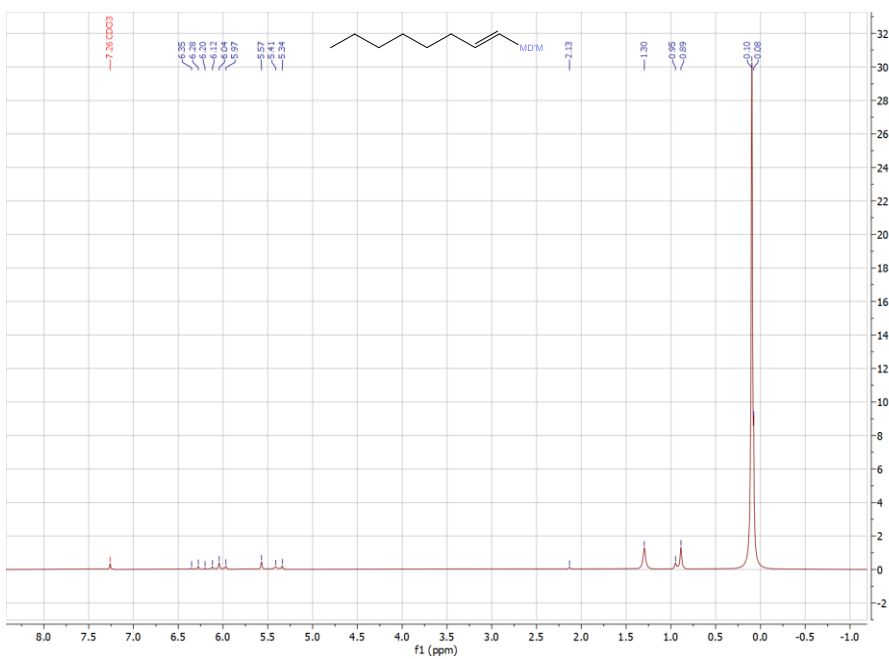


*Figure A4: $^1$H NMR (80 MHz, CDCl3, 298K) of phenylacetylene-MDM.*

94

*Figure A5: ¹H NMR (80 MHz, CDCl3, 298K) of 1octyne-MDM.*